Translation of ligand binding to activation in olfactory cyclic nucleotide-gated (CNG) channels

Dissertation

zur Erlangung des akademischen Grades

Doctor of Philosophy (Ph.D.)

vorgelegt dem Rat der Medizinischen Fakultät
der Friedrich-Schiller-Universität Jena

von Nisa Wongsamitkul

geboren am 08.09.1983 in Saraburi, Thailand

Gutachter:

1. Prof. Dr. med. Klaus Benndorf. Universitätsklinikum Jena, Jena
2. Prof. Dr. Ingo Dahse. Friedrich-Schiller-Universität Jena, Jena
3. Prof. Dr. Stephan Frings. Universität Heidelberg, Heidelberg

Tag der öffentlichen Verteidigung: 06.10.2015

Contents

1. Summary

Cyclic nucleotide-gated (CNG) channels play a fundamental role in the transduction of olfactory sensory neurons. Olfactory CNG channels are heterotetramers composed of three different subunits, CNGA2, CNGA4 and CNGB1b, with a stoichiometry 2:1:1. When heterologously expressed, only the CNGA2 subunits can form functional homotetrameric channels. Up to now, it is still unclear even in the simplest structure of homotetrameric CNGA2 channels, how ligand binding is translated to channel gating in the individual subunit. Therefore, we aimed to characterize the work of only one CNGA2 subunit from ligand binding to activation gating in homotetrameric CNGA2 channels. As tools, the concatenation technique in combination with the conventional patch clamp technique were used. The concatenation technique allowed us to control the number and the position of the functional subunits. Selected subunits were rendered almost insensitive to cGMP by a point mutation of an arginine residue to glutamate (R538E) in the binding domain. In this study we termed a wild-type subunit as *wt* and a mutated subunit as *mut*. With this approach we observed and characterized the contribution of individual subunits to channel activation.

First, we show direct evidence indicating that the CNGA2 concatemeric channels function properly: 1) Based on macroscopic-current studies, the concentration-response relationship of *wt*-*wt*-*wt*-*wt* concatemer was almost identical to that of channels formed by non-concatenated subunits (4*wt*). 2) When coexpressing *wt*-*wt*-*wt*-*wt* concatemer with *mut* subunits, the concentration-response relationship was indistinguishable from that of *wt*-*wt*-*wt*-*wt* concatemer alone. 3) The amplitude of the single-channel current and the open probability of *wt*-*wt*-*wt*-*wt* channels were not significantly different from that of 4*wt* channels in the presence of saturating cGMP concentrations. These findings confirm that the concatenation technique does not have any effect on channel function.

Then, the concatemers containing 1, 2, 3 or 4 mutated subunits were electrophysiologically characterized. The respective concentration-response relationships showed that an increase of the number of *mut* subunits in the

concatemeric channels caused graded losses in cGMP sensitivity (EC_{50}) associated with a systematic decrease of the Hill coefficient (*H*). Moreover, by comparing the concentration-response relationships obtained from concatemers with either one *wt*-subunit or from concatamers with two *wt*-subunits we showed that the position of the functional subunit(s) in the concatemers is irrelevant for the channel function.

We further characterized the CNGA2-channel activation induced by the first ligand binding step in *mut-mut-mut-wt* channels by means of the single-channel recordings and a global fit analysis of all five concatemers (*wt-wt-wt-wt*, *mut-wt-wt-wt mut-mut-wt-wt*, *mut-mut-mut-wt*, *mut-mut-mut-mut)* with five Markovian models. We found that already the first binding step can trigger noticeable channel activity with the channel reaching to the full conductance state. This suggests that the second, third and fourth binding steps influence only the channel open probability.

Furthermore, the open probability for the *mut-mut-wt-wt* channels obtained not only from the measured single-channel data but also that predicted by the Markov model suggest that the second binding step is the most important event for channel activation because this step drives the channel from the closed to the maximal open state. Together, these results provide direct information about the functional role of individual subunits in homotetrameric CNGA2 channels. This approach may be successfully applied in other ion channels and receptors for studying the role of subunits in homomeric as well as in heteromeric channels.

Zusammenfassung

Durch zyklische Nukleotide gesteuerte Kanäle (CNG-Kanäle) spielen eine tragende Rolle in der Signaltransduktion in olfaktorischen Sensorneuronen. Olfaktorische CNG-Kanäle sind Heterotetramere, die sich aus drei Typen von Untereinheiten zusammensetzen, CNGA2, CNGA4 und CNGB1b, die im Verhältnis 2:1:1 vorliegen. Wenn sie in heterologen Systemen exprimiert werden, können die CNGA2-Untereinheiten allein funktionelle homotetramere Kanäle bilden. Bis jetzt ist es aber nicht klar, selbst in der einfachsten Struktur homotetramerer CNGA2-Kanäle, wie die Ligandenbindung in die Kanalöffnung in den einzelnen Untereinheiten übersetzt wird. Daher war es unser Ziel, die Arbeit einer einzelnen CNGA2-Einheit von Ligandenbindung bis Aktivierungs-Gating in homotetrameren CNGA2-Kanälen zu charakterisieren. Als Werkzeuge wurden die Konkatenierungstechnik in Kombination mit der herkömmlichen Patch-Clamp-Technik verwendet. Die Konkatenierungstechnik ermöglicht es uns, die Anzahl und die Position der funktionellen Einheiten zu steuern. Ausgewählte Untereinheiten wurden durch eine Punktmutation eines Argininrests auf Glutamat (R538E) in der Bindungsdomäne fast unempfindlich gegen cGMP. In dieser Arbeit wird eine Wildtyp-Untereinheit als *wt* und eine mutierte Untereinheit als *mut* bezeichnet. Mit dieser Vorgehensweise haben wir den Beitrag der einzelnen Untereinheiten an die Kanalaktivierung beobachtet und charakterisiert.

Zuerst zeigen wir direkte Beweise dafür, dass die konkatemeren CNGA2-Kanäle ordnungsgemäß funktionieren: 1) Basierend auf Untersuchungen des makroskopischen Stroms, war die Konzentrations-Wirkungs-Beziehung des *wt*-*wt*-*wt*-*wt*-Konkatemers fast identisch mit der des aus nicht-verketteten Untereinheiten gebildeten Kanals (*4* wt). 2) Bei Koexpression von *wt*-*wt*-*wt*-*wt* Konkatemer mit *mut* Untereinheiten war die Konzentrations-Wirkungs-Beziehung nicht von der des *wt*-*wt*-*wt*-*wt*-Konkatemers allein unterscheidbar. 3) Die Amplitude des Einzelkanalstroms und der Öffnungswahrscheinlichkeit von *wt*-*wt*-*wt*-*wt* Kanälen waren nicht signifikant verschieden von 4 *wt*-Kanälen in Gegenwart sättigender

Konzentrationen von cGMP. Diese Ergebnisse bestätigen, dass die Konkatenierungstechnik keinerlei Auswirkungen auf die Kanalfunktion aufweist.
Anschließend wurden die Konkatemere, die 1, 2, 3 oder 4 mutierte Untereinheiten enthielten, elektrophysiologisch charakterisiert. Die jeweiligen Konzentration-Wirkungs-Beziehungen haben gezeigt, dass eine Erhöhung der Anzahl von *mut*-Untereinheiten in den konkatemeren Kanälen abgestufte Verluste der cGMP-Empfindlichkeit (EC_{50}) verursacht, denen eine systematische Abnahme des Hill-Koeffizienten (*H*) zugeordnet ist. Weiterhin kann durch Vergleichen der Konzentrations-Wirkungs-Beziehungen von Konkatemeren mit entweder einer *wt*-Untereinheit oder von Konkatemeren mit zwei *wt*-Untereinheiten gezeigt werden, dass die Position der funktionellen Einheit(en) in den Konkatemeren irrelevant ist für die Kanalfunktion.
Weiterhin haben wir die durch den ersten Ligandenbindungsschritt in *mut-mut-mut-wt*-Kanälen induzierte CNGA2-Kanal-Aktivierung durch Einzelkanalaufnahmen und eine globale Anpassung aller fünf Konkatemere (*wt-wt-wt-wt, mut-wt-wt-wt, mut-mut-wt-wt, mut-mut-mut-wt, mut-mut-mut-mut*) mit fünf Markov-Modellen charakterisiert. Wir haben festgestellt, dass bereits der erste Bindungsschritt bemerkbare Kanalaktivität, mit der der Kanal die volle Leitfähigkeit erreichen kann, auslösen kann. Dies deutet darauf hin, dass der zweite, dritte und vierte Bindungsschritt nur die Kanalöffnungswahrscheinlichkeit beeinflusst. Darüber hinaus lässt die Offenwahrscheinlichkeit für den *mut-mut-wt-wt* Kanal, die nicht nur aus den gemessenen Einzelkanaldaten, sondern auch durch das Markov-Modell vorhergesagt wurde, vermuten, dass der zweite Bindungsschritt das wichtigste Ereignis für die Kanalaktivierung ist, weil dieser Schritt den Kanal aus dem geschlossenen in den maximal offenen Zustand treibt. Zusammen liefern diese Ergebnisse direkte Informationen über die funktionelle Rolle der einzelnen Untereinheiten in homotetrameren CNGA2-Kanälen. Dieser Ansatz kann erfolgreich in anderen Ionenkanälen und Rezeptoren für die Untersuchung der Rolle von Untereinheiten in homomeren sowie heteromeren Kanälen angewendet werden.

2. Introduction

2.1. Cyclic nucleotide-gated (CNG) channels

2.1.1. Overview of CNG channels

Cyclic nucleotide-gated (CNG) channels are nonselective cation channels whose activation is mediated by the direct binding of intracellular cyclic nucleotides (guanosine 3':5'-cyclic monophosphate (cGMP) and adenosine 3':5'-cyclic monophosphate (cAMP), thereby mediating influx of Na^+ and Ca^{2+} ions into the cells, leading finally to depolarization. CNG channels are important for the signal transduction pathways of photoreceptors and olfactory sensory neurons (Craven and Zagotta 2006). In 1985, Fesenko and his colleagues first discovered that cGMP directly activates CNG channels in the plasma membrane of retinal rod outer segments, where they play a crucial role in phototransduction (Fesenko et al. 1985). CNG channels were also identified in the outer segment membrane of catfish cone photoreceptors (Haynes and Yau 1985). In 1987, Nakamura and Gold found a channel directly gated by cGMP or cAMP in the cilia of olfactory sensory neurons (Nakamura and Gold 1987). The first gene encoding a CNG channel subunit of bovine retinal rods was first cloned by Kaupp and his coworkers, thereby initiating the investigation of the physiological and biophysical properties of these channels at molecular level (Kaupp et al. 1989). CNG channels have also been identified in a variety of other neuronal and non-neuronal cells and tissues such as brain, testis, kidneys and heart (Kaupp and Seifert 2002). However, the physiological function of CNG channels in most of these cells is still unclear.

Later, CNG channels have been identified also in invertebrates including *Caenorhabditis elegans*, *Drosophila melanogaster*, and *Limulus polyphemus*, but their functions remain largely unknown. In *Caenorhabditis elegans*, it has been shown that tax-2 and tax-4 encoding CNG channels are critical for chemosensing and thermosensing (Coburn and Bargmann 1996, Komatsu 1996).

2.1.2. Structure and basic properties of CNG channels

CNG channels belong to a heterogeneous gene superfamily of ion channels sharing a common transmembrane topology, and pore structure and a cyclic nucleotide-binding domain (CNBD) located in the C-terminus (Kaupp and Seifert 2002). Other members of this superfamily are hyperpolarization-activated cyclic nucleotide-gated (HCN) channels (Kaupp and Seifert 2001), the ether-a-gogo (EAG), human eag-related gene (HERG) family of K^+ channels (Ganetzky et al. 1999) and plant inward rectifying K^+ channels (KAT, AKT and KST channels) (Schachtman 2000). Despite the fact that CNG channels are only weakly voltage dependent (Karpen 1988), they belong to the superfamily of voltage-gated ion channels and the primary amino acid sequence of CNG channels is highly homologous to the voltage-gated K^+ channel family (Jan and Jan 1990). Like voltage-gated K^+ channels, CNG channels are thought to exist as tetramers consisting of four subunits arranged around a central pore (Liu et al. 1996). All subunits of CNG channels contain a cytoplasmic N-terminus, six transmembrane segments (S1-S6) including a positively charged S4 segment, a reentrant pore loop (P loop) linking the S5 and S6 transmembrane segments and a cytoplasmic C-terminus. The C-terminal region contains a highly conserved region known as C-linker followed by a CNBD (Kaupp and Seifert 2002) (Figure 1). The CNBD has been conserved in several proteins, including cAMP and cGMP- dependent protein kinases (PKA and PKG, respectively) (Pfeifer et al. 1999), bacterial transcription factors (Weber et al. 1987) and cAMP- dependent guanine nucleotide exchange factors (Bos 2006).

CNG channels are activated by the direct binding of intracellular cyclic nucleotides, including cGMP and cAMP, to the CNBD with accommodation of only one cGMP or cAMP molecule per subunit (Zagotta and Siegelbaum 1996). The degree of ligand discrimination differs significantly between each cell type. CNG channels in photoreceptors are able to efficiently discriminate between cGMP and cAMP whereas in olfactory sensory neurons they are similarly sensitive to both ligands (Tanaka et al. 1989, Frings et al. 1992).

There are three domains that are involved in CNG channel activation: (1) the CNBD in the C-terminal region (Kaupp et al. 1989), (2) the C-linker which allosterically couples the ligand binding and channel gating (Zong et al. 1998, Paoletti et al. 1999, Gordon and Zagotta 1995) and (3) the distal region of the S6 segment (Giorgetti et al. 2005).

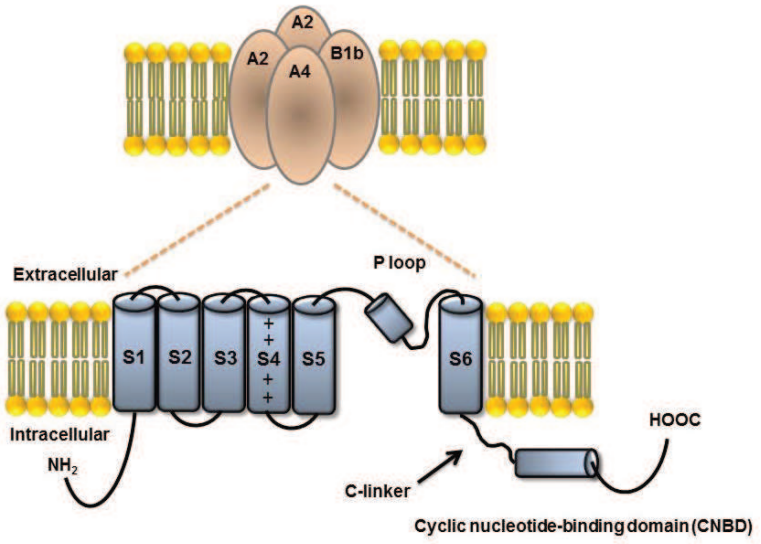

Figure 1. Cartoon of the CNG channel structure. Olfactory CNG channels are tetramers containing 3 different subunits 2xCNGA2: 1xCNGA4: 1xCNGB1b (as shown in the upper panel). Each subunit contains six transmembrane domains (S1-S6). The S4 domain is positively charged. The pore region (P loop) is situated between the S5 and S6 domains. The C-terminus of all subunits contains a cyclic nucleotide-binding domain (CNBD) that is linked to the end of S6 segment by the C-linker region. Both N-terminus and C-terminus are located at the intracellular side (as shown in the lower panel).

Currently, the family of mammalian CNG channels is composed of six homologous members including CNGA1, CNGA2, CNGA3, CNGA4, CNGB1a/b and CNGB3. (Kaupp and Seifert 2002). CNGA and CNGB subunits are also identified in the genome of some invertebrates (e.g. *Caenorhabditis elegans*, *Drosophila melanogaster*), indicating a former segregation of these two subunits in evolution (Biel and Michalakis 2007). When CNGA1, CNGA2 and CNGA3 subunits are expressed alone in heterologous systems (HEK293 cells or *Xenopus* oocytes), they can form functional channels by themselves. Nevertheless, functional

characteristics of these homotetrameric channels such as single current properties, cyclic nucleotide affinity, permeation properties and regulation by Ca^{2+}, are different from those of native channels (Kaupp and Seifert 2002). In contrast to the other three CNGA subunits, CNGA4 subunits are not able to form functional homotetrameric channel due to the fact that its C-linker contains a tripeptide (Phenylalanine-Proline-Asparagine) that dramatically reduces the efficacy of ligand gating (Zhou et al. 2004). Also, CNGB1 and CNGB3 subunits cannot form functional channels by themselves (Bradley et al. 1994). However, when coexpressing CNGB subunits with CNGA1-CNGA3, these subunits generate unique properties including single-channel flickering and increased cAMP sensitivity. The functional characteristics of these heterotetrameric channels are similar to that of native channels, suggesting that native CNG channels are heterotetrameric proteins (Bradley et al. 1994, Liman and Buck 1994). In addition, splicing variants have been identified in rod photoreceptors (CNGB1a) and in olfactory sensory neurons (CNGB1b) (Korschen et al. 1995, Sautter et al. 1998, Bonigk et al. 1999).

The precise subunit stoichiometry of CNG channels has been investigated by means of biochemical and fluorescence resonance energy transfer (FRET) techniques. The CNG channel from rod photoreceptors consists of two types of subunits: CNGA1 and CNGB1a (Kaupp et al. 1989, Chen et al. 1993) with a stoichiometry three CNGA1 and one CNGB1a (Weitz et al. 2002, Zhong et al. 2002, Zheng et al. 2002). The CNG channel from cone photoreceptors is composed of two types of subunits: CNGA3 and CNGB3 (Bonigk et al. 1993, Gerstner et al. 2000) with a stoichiometry two CNGA3 and two CNGB3 (Peng et al. 2004). The native olfactory CNG channel contains three types of subunits: CNGA2, CNGA4 and CNGB1b (Dhallan et al. 1990, Ludwig et al. 1990, Bradley et al. 1994, Liman and Buck 1994) with a stoichiometry of two CNGA2, one CNGA4 and one CNGB1b (Zheng and Zagotta 2004) (Figure 2).

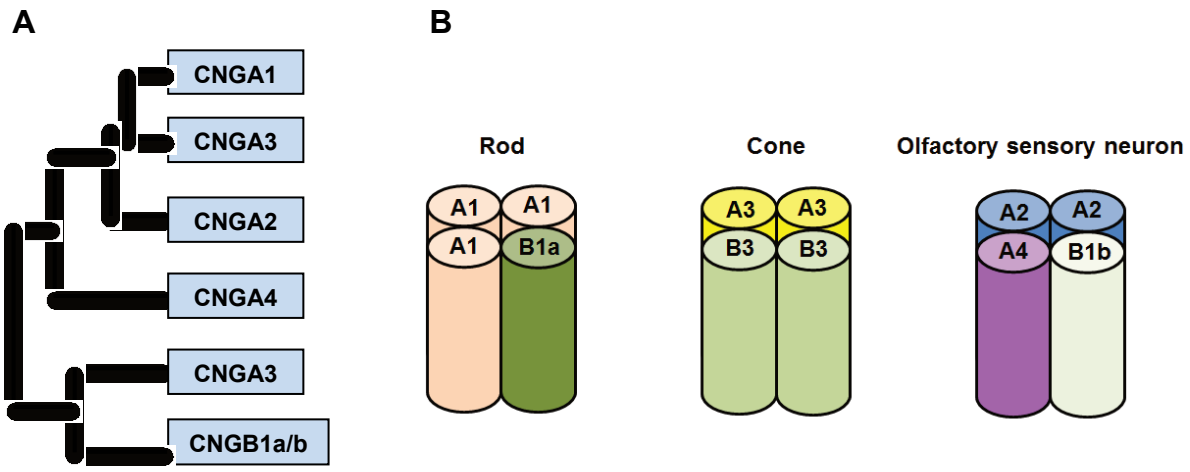

Figure 2. CNG channels from retinal photoreceptors and olfactory sensory neurons
A) Phylogenic tree of mammalian CNG channel subunits. B) Subunit stoichiometry of CNG channels from rod photoreceptors (left), cone photoreceptors (middle) and olfactory sensory neurons (right).

2.1.3. Role of CNG channels in olfactory sensory neurons

The olfactory system is very important for organisms, enabling them to detect and discriminate a large number of low molecular mass, mostly organic compounds called odorants. Olfactory transduction in vertebrates relies on the function of CNG channels which are expressed in the cilia of olfactory sensory neurons (OSNs) of the main olfactory epithelium. The cilia, which are covered by a thin layer of mucus, contain all molecular components responsible for chemotransduction and act as the primary interface between odorants in the external environment and the nervous system (Firestein 2001). When an odorant molecule binds to its odorant receptor (OR) (Buck and Axel 1991), this initiates a G-protein (an olfactory specific subtype, G_{olf})-mediated signaling cascade (Jones and Reed 1989), leading to activation of a ciliary adenylyl cyclase (AC) (Bakalyar and Reed 1990). The activated adenylyl cyclase causes a rapid increase in the intracellular cAMP level by concerting the ATP molecule into cAMP. cAMP binds and activates the CNG channel that allows mainly Na^+ and Ca^{2+} to enter the cell under physiological

conditions (Nakamura and Gold 1987, Frings et al. 1995). The influx of positive charges through the CNG channels leads to cell depolarization (Nakamura and Gold 1987). Moreover, the influx of Ca^{2+} activates the Ca^{2+}- activated Cl^- channel (ClC_{Ca}) (Kleene and Gesteland 1991), resulting in a stronger membrane depolarization. The Ca^{2+}- ions entering the cell have also a modulatory effect on the olfactory signal transduction (Kurahashi and Menini 1997). Fast odor adaptation is caused by the binding of Ca^{2+}-activated Calmodulin (Ca^{2+}/CaM) to specific binding sites located at the N-terminus of the modulatory subunits, resulting in a reduction of the ligand sensitivity of the CNG channels (Menini 1999). In addition, to regulate CNG channels, the Ca^{2+}/CaM complex also activates a phosphodiesterase (PDE) that hydrolyzes cAMP to AMP (Borisy et al. 1992, Yan et al. 1995). Ca^{2+} ions are extruded by a Na^+-Ca^{2+} exchanger (NCX) in order to maintain the low levels of intracellular Ca^{2+} concentration (Kaneko et al. 2004). Both inhibitory mechanisms contribute to olfactory adaptation to long odorant exposure. Olfactory signal transduction is shown in Figure 3.

Moreover, olfactory CNG channels expressed in heterologous systems are also directly inhibited by phosphatidylinositol-3, 4, 5-trisphosphate (PIP_3) by interfering with an autoexcitatory interaction between the N-and C-termini of adjacent subunits (Brady et al. 2006). Some reports suggest that PIP_3 may reduce olfactory CNG channel sensitivity in the presence of complex odorants but the underlying mechanism is still unclear (Brady et al. 2006, Spehr et al. 2002). In addition to activate CNG channels by cyclic nucleotides, it has been shown that odorant molecules itself may directly inhibit the olfactory CNG channels (Chen et al. 2006).

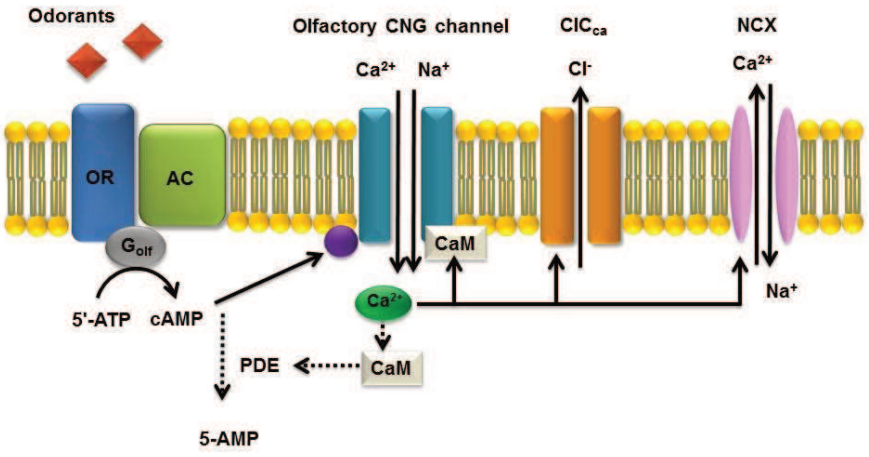

Figure 3. Olfactory signal transduction. The odorants bind to odorant receptor (OR) located in the cilia of olfactory sensory neurons. The activated G-protein (G_{olf}) stimulates an adenylate cyclase (AC), resulting in an increase of intracellular cAMP. cAMP binds and opens the CNG channel which transports Na^+ and Ca^{2+} into the cells. The inward current depolarizes the membrane. The increased intracellular Ca^{2+} opens a Ca^{2+}-activated Cl^- channel (ClC_{Ca}), leading to Cl^- efflux which further depolarizes the cell. In addition, Ca^{2+} binds to calmodulin (CaM), lowering the ligand sensitivity of the CNG channels and also activates a phosphodiesterase (PDE) leading to the termination of the olfactory response. Ca^{2+} is transported out of the cell by a Na^+-Ca^{2+} exchanger (NCX).

2.1.4. Molecular mechanism of CNG-channel gating

CNG channels are membrane proteins forming ion-selective permeable pores through plasma membranes and have two well-defined channel states: the open state and the closed state. In the open state, CNG channels are permeable for monovalent ions moving passively into the cells, whereas in the closed state the pore is blocked, therefore ion conduction does not occur. The study of the relationship between ligand binding and channel gating and also the crucial role of individual subunits in response to this process have long been a goal of ion channel research. However, the molecular mechanism of translation of ligand binding to channel gating is not fully clear.

Therefore, there are several constantly evolving kinetic models used for describing the ligand binding to CNG channel activation: (1) the linear model or the sequential model (Karpen et al. 1988); (2) the Monod-Wyman-Changeux (MWC) model (Monod et al. 1965); (3) the coupled dimer (CD) model (Liu et al. 1998); (4) the C4L- and C3L-model (Biskup et al. 2007, Nache et al. 2005), and (5) the C4L-*O4L-model (Nache et al., 2013).

The linear model is the simplest kinetic model used to describe the CNG channel gating. According to this model, cyclic nucleotides bind sequentially, followed by a final transition from the closed to the open state when the channel is fully liganded (Karpen et al. 1988). It has been assumed that there are only two channel states, open and closed. Furthermore, the model indicates that the channel transition from closed to open state is very rapid and weakly voltage dependent. This model can be used to explain the kinetic and steady-state behavior of CNG channels activated by various cyclic nucleotide concentrations. However, it was subsequently found that CNG channels can open also in the absence of ligand (Kleene 2000, Picones and Korenbrot 1995), thus this model is not sufficient to explain the channel behavior.

The Monod-Wyman-Changeux (MWC) model (also known as a cyclic allosteric model) was originally used to describe the cooporative behavior of hemoglobin (Monod et al. 1965). Generally, this model allows for the channel to open whether it is unliganded, partially liganded, or fully liganded. The channel undergoes a concerted conformational transition from the closed state to the open state. This transition is energetically stabilized by a constant amount for each ligand bound. Despite reproducing the activation of CNG channels by cyclic nucleotides, this model is limited because it does not predict the experimentally observed open probabilities for partially liganded channels (Ruiz and Karpen 1999). In addition, this model is inadequate, since it does not only predict sigmoidal instead of exponential activation time course, but also shows a higher level of binding than activation at all ligand concentrations (Nache et al. 2005).

The coupled-dimer (CD) model was proposed in order to overcome previous limitations of the MWC model. The CD model arose from experiments designed to

examine the energetic contribution of binding successive ligands to CNG and HCN channels (Liu et al. 1998, Ulens and Siegelbaum 2003). This model assumes that CNG tetrameric channel contains two functional dimers and each dimer undergoes an independent allosteric transition between a resting and active state which is coupled to an increase in the affinity of each subunit to cyclic nucleotide. Maximal channel opening occurs only when both dimers are in active state.

The C3L model was proposed by our group (Nache et al. 2005). In this model, the activation of olfactory CNG channels was determined by photolysis-induced jumps of cGMP or cAMP. The C3L model containing three binding sites with a ligand affinity high-low-high, indicates that the binding of only three ligands is required to describe the activation time courses and that the ligand binding is highly cooperative. However, there is still to be shown whether the cooperativity is caused by the binding, the gating, or both and what the function of the fourth subunit is.

We later extended the C3L model and developed a more accurate kinetic scheme for the homotetrameric CNGA2 channels, the C4L model. In this study, the binding of the ligand and the activation of channels were simultaneously investigated by using the confocal patch-clamp fluorometry (Biskup et al. 2007). The C4L model includes 4 binding steps and shows a significant interaction between the binding sites. The second binding step already generates a switch from a mostly closed to fully open state, whereas the third and the fourth binding step only stabilizes the open channel (Biskup et al. 2007).

The C4L-*O4L model was proposed later by performing a global analysis of the ligand binding/unbinding and CNGA2 channel activation/deactivation experimental data. The C4L-*O4L model described two pathways for ligand unbinding: the partially liganded CNGA2 channel unbinds its ligands from closed states only while the fully liganded channel reaches a different open state, thereby allowing a very rapid unbinding of all four ligands. The consequent transition pathway for ligand binding and activation of a fully liganded channel is different from that of ligand unbinding and deactivation. This finding results in pronounced hysteresis in the CNGA2 channel gating mechanism (Nache et al. 2013).

2.1.5. Olfactory CNG knockout models and human channelopathies

At present, the studies of gene knockout in mice and the analysis of human diseases caused by mutations in CNG channel genes, as referred to CNG channelopathies, have obviously increased our knowledge about the physiological role of CNG channels in the olfactory system (Biel and Michalakis 2007). This section represents a summary of the effects of some mutations in the gene encoding olfactory CNG subunits in mice models. Native olfactory CNG channels contain three different types of subunits, the principal CNGA2 subunit and two modulatory CNGA4 and CNGB1b subunits with a stoichiometry 2:1:1 (Zheng and Zagotta 2004). Unlike other CNG channel genes, the CNGA2 gene is located on the X chromosome. There are several studies on mice showing that four different CNGA2-knockout mouse lines have been produced in order to describe the physiological role of this subunit (Baker et al. 1999, Brunet et al. 1996, Zheng et al. 2000). By using electroolfactrogram recordings (EOG), it has been shown that CNGA2-knockout mice exhibit no detectable responses to odorants (Brunet et al. 1996). Furthermore, using perforate patch-clamp configuration on OSNs from mice defective for the CNGA2 subunit, no response to odorants or cAMP activators (e.g., IBMX and forskolin) was observed (Delay and Restrepo 2004). These findings strongly suggest that the transduction mechanism mediating odorant detection is conferred by a cAMP/CNGA2 signaling pathway. The CNGA2 subunit also plays a crucial role in the normal development of olfactory epithelium and olfactory bulb. The olfactory epithelium is thinner and the olfactory bulb is of smaller size in CNGA2-knockout mice in comparison to wild-type mice (Baker et al. 1999). Mice lacking functional CNGA2s also show both abnormal sexual and aggressive behaviors, suggesting a broad and important role for CNGA2 subunits in regulating these behaviors (Mandiyan et al. 2005).

CNGA4-deficient mice displayed an unusual reduction in the rate of the electrophysiological response to odors due to defective Ca^{2+}-calmodulin mediated channel desensitization (Munger et al. 2001). Also, the channel's affinity for cAMP

decreased, with a dose-response curve shifted ~10-fold to higher concentrations, indicating that the mouse CNGA4 subunit is required for acceleration of Ca^{2+}-calmodulin-dependent odor adaptation of OSNs. The behavioral testing in CNGA4-deficient mice showed a significantly increased odorant-detection threshold, consistent with the reduced cAMP affinity observed in the heterologous expression systems (Kelliher et al. 2003). Moreover, these mice were profoundly less effective to detect and discriminate olfactory stimuli in the presence of adapting background odors. These findings demonstrate the fundamental role of CNGA4 subunits in odor discrimination and adaptation behaviors (Kelliher et al. 2003). In contrast to CNGA2-deficient mice, the olfactory epithelium and the olfactory bulb develop normally in CNGA4-deficient mice. Moreover, these knockout mice are fertile and show no obvious morphological changes compared with wild-type mice (Kelliher et al. 2003, Munger et al. 2001).

CNGB1b-deficient (CNGB1b-/-) mice displayed a severely impaired olfactory performance and their EOG responses showed a reduced maximal amplitude and a decelerated onset and recovery kinetics in comparison to wild-type mice (Michalakis et al. 2006). Electrophysiological measurements of OSNs obtained from CNGB1b-knockout mice showed different biophysical properties compared with those of wild-type mice including: low CNG current with decreased cAMP sensitivity, very rapid flickering of channel gating and slow Ca^{2+}-calmodulin modulation. Moreover, the CNGA2/CNGA4 channel in CNGB1b-knockout mice was targeted to the plasma membrane of the olfactory knob and failed to reach the olfactory cilia. The defective trafficking was also observed in CNGA4-deficient mice (Michalakis et al. 2006). This suggests that the CNGB1b together with the CNGA4 subunit is required for ciliary targeting of the olfactory CNG channel (Michalakis et al. 2006). CNGB1b-knockout mice also show an increases postnatal mortality and reduced body weight as a result of impaired exploratory activities such as nursing and food intake (Michalakis et al. 2006).

2.2. The concatenation technique

The simplest definition of subunit concatenation is that two or more subunits are covalently linked together by introducing a linker or linkers, or new protein sequence between subunits. Over the past 10 years the concatenation technique has been used to study the structure and the function of numerous multimeric proteins, including receptors and ion channels (Sack et al. 2008). The concatenation technique appeared as a necessity when studying heterotetrameric proteins. It is not an easy task to gain insight into the stoichiometry and arrangement of subunits and their functional roles only by recombinant expression of mixtures of single subunits due to the different subtypes of ion channels or receptors with different stoichiometry or arrangements can be formed (Minier and Sigel 2004). Therefore, the concatenation technique represents an alternative approach for understanding subunit composition and their arrangement.

This method forces subunits to be in a particular stoichiometry by covalently linking the subunits at the DNA level in order to predetermine their alignment. Technically, to obtain concatenated subunits, the 3' stop codon from the initial subunits is removed and then a linker is inserted to the 5' end of the following subunit's sequence. This resulting protein thus has the C-terminus of the initial subunit covalently linked to the N-terminus of the following subunit. These contiguous proteins are commonly known as tethered, tandem, linked, or concatenated (Sack et al. 2008).

Also, the properties of the linker have to be considered. For example: the formation of the linker sequence as a secondary structure is an undesirable effect because this might increase the required length of the concatameric construct (Minier and Sigel 2004). The length of the linker is also of importance. It has been shown for the pentameric $GABA_A$ channels that if the linkers are too short, the channels do not function (Baumann et al. 2001). In contrast, when using very long linkers to link two subunits in the nicotinic acetylcholine receptor, this linkage allows assembly of two functional dipentamers resulting in variable stoichiometries (Zhou et al. 2003).

2.2.1. The concatenation technique in ion channel research

The use of the concatenation technique was first applied to voltage-gated K^+ channels (K_v) in order to test whether K^+ channels are heteromultimeric channels (Isacoff et al. 1990). Since then this technique has been successfully used in many other studies on K^+-channels, for examples (1) to characterize the subunit stoichiometry and the quaternary structure of voltage-gated K^+ channels (K_v) and of inwardly rectifying K^+ channels (K_{ir}) (Silverman et al. 1996, Tu and Deutsch 1999, Yang et al. 1995); (2) to study the gating mechanism of K_v channels (RBK1, ratK_V1.1) (Hurst et al. 1992, Tytgat et al. 1993); (3) to determine the positional effects of specific subunits on the functional properties of heterotetrameric K_{ir} channels (Pessia et al. 1996) (4) to characterize the activation and inactivation mechanisms in the mammalian shaker K^+ channel (K_v1.4) (Lee et al. 1996); (5) to identify the effects of point mutations in specific subunits on K_v-channel function (Hurst et al. 1992, Kirsch et al. 1995).

The concatenation technique was also applied to other ion channels and receptors, including the hyperpolarization-activated cyclic nucleotide-sensitive (HCN) ion channels (Ulens and Siegelbaum 2003), the epithelial Na^+ channels (ENaC) (Firsov et al. 1998), the Cystic Fibrosis Transmembrane Conductance Regulator (CFTR) channels (Zerhusen et al. 1999), the mechanosensitive channel protein of *E. coli* (Blount et al. 1996), the $P2X_2$ receptors (Newbolt et al. 1998), the pentameric ligand-gated $GABA_A$ receptors (Baur et al. 2006), the aquaporins (Mathai und Agre 1999), transport proteins (e.g., Na^+ pump and lactose permease) (Emerick and Fambrough 1993, Sahin-Toth et al. 1994).

The concatenation method has also been applied to CNG channels from both, rod photoreceptors and olfactory sensory neurons, in order to gain insight into the stoichiometry and the arrangement of the channel subunits (Varnum and Zagotta 1996, Liu et al. 1998, Shapiro und Zagotta 1998, Morrill and MacKinnon 1999, He et al. 2000).

Nevertheless, there is evidence showing that the subunit concatenation hinders the channel proper function for reasons that are currently still unclear. For example,

concatenated $P2X_1$ receptors are not functional. Although they were already synthesized in oocytes, they were retained mainly as aggregates in the endoplasmic reticulum (Nicke et al. 2003). In contrast, $P2X_2$ concatemers can form fully functional channels in the plasma membrane (Stelmashenko et al. 2012). There is also evidence showing that the concatenation can disrupt the normal assembly of subunits, and that the subunits from different concatemers may join together to form one ion channel, whereas adjacent subunits are excluded from the channel (Zhou et al. 2003).

2.2.2. Validation of proper assembly and stoichiometry of expressed concatemers

Up to now, it has not been reported proteolysis of concatemers in the literature. In principle, proteolysis could occur either within a subunit or within the linker and may lead to unexpected results: (1) an underestimation of the expression level of the resulting construct if the concatemeric constructs are broken down in smaller side products, or (2) incorrect interpretation of obtained results if the proteolysis affects the linker sequence and this can lead to products that are able to form functional channels in the plasma membrane (Minier and Sigel 2004).

Therefore, in order to ensure that the concatemeric channels are properly assembled and that they comprise only the expected subunits, different strategies comprising biochemical tests and/or functional electrophysiological controls were performed. To test whether the concatemers remain intact in the plasma membrane, the size of expressed concatenated proteins could be for example investigated (Sack et al. 2008).

Several biochemical methods have been used to test truncated concatemers. For examples: 1) Western blotting is a common method which is regularly used to prove the integrity of the concatemers in the plasma membrane. This technique was used to confirm that the K_v1-concatemeric constructs expressed in HEK293 cells have the correct sizes and subunit compositions (Sokolov et al. 2007). Similar tests were also applied for the concatemeric pentameric constructs of neuronal

nicotinic acetylcholine receptors and in this way was certified that the linked subunits have the appropriate length (Groot-Kormelink et al. 2006). 2) Surface biotinylation is used to detect whether the concatemers are intact. For instance, determination of heteromeric Kv1 concatemers expressed in CHO cells by using surface biotinylation indicated that the plasma membrane concatenated channels are still intact (Akhtar et al. 2002).

An alternative to biochemical methods for assessing the integrity of the concatenated subunits is the characterization of the electrophysiological properties of the concatemeric constructs. For example, Groot-Kormelink and co-workers suggested that the functional studies (the electrophysiological testing) are more sensitive than any other methods in detecting the presence of broken products and/or incomplete concatemer assembly. Moreover, these tests would detect only those channels that are functional on the plasma membrane. The data obtained from dose-response relationships indicated that neuronal nicotinic receptors formed by the pentameric concatemeric construct have ACh sensitivity similar to that of receptors formed by monomeric constructs (Groot-Kormelink et al. 2006). Furthermore, the conductance-voltage (g-V) relationship is a standard method used to validate the proper assembly of concatemeric voltage-gated channels. If g-V plot well fit by a single Boltzmann distribution, this means that the channels have an only one uniform population. Whereas, a complicated g-V plot suggests multiple populations of channels (Sack et al. 2008).

3. Objectives

Cyclic nucleotide-gated (CNG) channels play an important role in the olfactory signal transduction (Kaupp and Seifert 2002). Olfactory CNG channels are heterotetrameric proteins composed of three different subunits, CNGA2, CNGA4 and CNGB1b, with a stoichiometry 2:1:1 (Zheng and Zagotta 2004). When heterologously expressed, only the CNGA2 subunits can form functional homotetrameric channels. Nevertheless, when coexpressed with the CNGA2 subunit, the CNGA4 and CNGB1b function as modulatory subunits by conferring a number of important physiological characteristics onto the heterotetrameric channel (Bonigk et al. 1999, Munger et al. 2001, Sautter et al. 1998). The homotetrameric CNGA2 channels are very crucial for studying basic biophysical processes (Biskup et al. 2007, Nache et al. 2005) because of the simplicity in composition. Nevertheless, the translation of ligand binding to channel gating in more simple olfactory CNGA2 channels is still unclear. It has been known only that the subunits cooperate because the value of Hill coefficient in concentration-response relationships is either two (Dhallan et al. 1990) or more than two (Bonigk et al. 1999). Therefore, to answer the question how the first ligand binds to an empty channel, we investigated the work of individually-selected subunits in functional channels in the absence of cooperative effects by means of the concatenation technique combined with inside-out patch-clamp and fitted the data with Markovian models.

The present study had the following objectives:

1. To successfully apply the concatenation technique to the homotetrameric CNGA2 channels. Then, the assessment of the influence of subunit concatenation on channel activity. Also, control experiments were planned to confirm the proper incorporation of the respective constructs in the plasma membrane and that the concatemers had the expected subunit composition.

2. To describe the contribution of each individual subunit to the activation of the homotetrameric CNGA2 channel. To this respect, CNGA2 tetrameric concatemers containing 1, 2, 3 or 4 mutated binding sites (*mut-wt-wt-wt*, *mut-mut-wt-wt*, *mut-mut-mut-wt* and *mut-mut-mut-mut*) were constructed and the cGMP-induced activation of the respective channels was analyzed.

3. To characterize the interaction between neighbored channel subunits in the homotetrameric CNGA2 channel. Therefore, the effect of the position of the functional subunit(s), in CNGA2 concatemers containing a different number of mutated binding sites on channel function was systematically analyzed.

4. To characterize the contribution of the first binding step to the total open probability of the CNGA2 channel in *mut-mut-mut-wt* and identification of the contribution of the only one *wt* subunit in *mut-mut-mut-wt* to channel activation by global fit analysis with Markovian models.

5. To determine the contribution of the binding of the second ligand to channel activation the CNGA2 channel in *mut-mut-wt-wt* and to confirm a previous report showing that the second binding step is able to switch the channel from mostly closed to a fully open channel.

Characterizing the contribution of each subunit to the channel activation, the intersubunit interactions and the molecular processes leading to channel opening is an important step toward understanding the function of the CNG channels in our olfactory system.

4. Materials and Methods

4.1. Generation of DNA constructs cRNA preparation

The experiments were performed on rat olfactory CNGA2 (accession number AF126808). All DNA constructs for wild-type CNG channel subunits with high-affinity binding sites (*wt*) and for CNGA2 subunits mutated at the cyclic nucleotide binding domain with low-affinity binding sites (*mut*) as well as all dimeric and tetrameric CNGA2 constructs were generated by Karin Schoknecht and by Prof. Thomas Zimmer (Institute of Physiology II). The R538E point mutation shifts the sensitivity of the respective subunits to a higher cGMP concentration range but had little effect on channel opening after the binding of ligand (Tibbs et al. 1998). All cDNA constructs were subcloned into pGEMHEnew (Liman et al. 1992) downstream to the T7 promoter. The CNGA2 tetrameric concatemers were obtained by connecting CNGA2 subunits via the short linker sequence glycine-serine-alanine (GSA), thereby removing respective stop codon. Preparation of cRNA was done by Karin Schoknecht using the mMESSAGE mMACHINE® Kit from Ambion. The quality of the cRNA was checked by agarose gel electrophoresis. The cRNA concentration was adjusted to 0.2 µg/µl using a NanoDrop spectrophotometer, and 2 µl aliquots were stored at -80 °C.

In total the eleven concatemers were constructed as follows;

1. *wt-wt-wt-wt*
2. *mut-wt-wt-wt*
3. *mut-mut-wt-wt*
4. *mut-mut-mut-wt*
5. *mut-mut-mut-mut*
6. *wt-mut-wt-mut*
7. *mut-wt-mut-wt*
8. *wt-wt-mut-mut*
9. *wt-mut-mut-mut*
10. *mut-wt-mut-mut*
11. *mut-mut-wt-mut*

4.2. Preparation of *Xenopus laevis* oocytes and cRNA injection

Oocytes were extracted from the South African clawed *Xenopus laevis* adult female frog. The ovarian lobes were surgically obtained from the frogs under anesthesia with 0.3% 3-aminobenzoic acid ethyl ester and were transferred to a petri dish containing oocyte ringer (OR2) solution. During surgery, the condition of the frogs was carefully monitored to avoid distress or infection. Only stage V–VI oocytes (Dumont 1972) were collected and then incubated for 105 min with collagenase (3 mg/ml, Roche, Grenzach-Wyhlen, Germany) in OR2 solution at room temperature. After isolation and defolliculation, the oocytes were injected with 40-70 nl of cRNA specific for the respective channels within 2-7 hours after surgery by using glass micropipettes with 2.0 mm outer diameter and 1.6 mm inner diameter (Hilgenberg, Malsfeld, Germany). Until experimental use, within 5 days after injection, the oocytes were incubated in Barth's medium at 18 ^{o}C. The Barth's medium was changed every 24 hours. In the day of experiment, the oocyte vitelline membrane was manually removed before patching. The experimental procedures were approved by the authorized animal ethical committee of Friedrich Schiller University Jena.

4.3. Chemicals and solutions

The chemicals, cGMP and cAMP, used to activate the CNG channels were obtained from Sigma (Type I, Sigma, St. Louise, U.S.A.). The desired cyclic-nucleotide concentrations were obtained by diluting the respective stock solutions (50 mM) with KCl solution. For single-channel measurements, 200 µM niflumic acid (Sigma, St. Louise, U.S.A) was added in the pipette solution in order to block endogenous Ca^{2+}-activated Cl^{-} channels which are the most abundant channels of the oocytes (White und Aylwin 1990). All chemicals were of analytical grade.

KCl solution contains: 150 mM KCl, EGTA 1 mM, 5 mM HEPES, pH 7.4 (KOH)

Barth's medium contains: 84 mM NaCl, 1 mM KCl, 2.4 mM $NaHCO_3$, 0.82 mM $MgSO_4$, 0.41 mM $CaCl_2$, 0.33 mM $Ca(NO_3)_2$, 7.5 mM TRIS, Cefuroxim, Penicillin/ Streptomycin, pH 7.4 (HCl)

OR2 solution contains: 82.5 mM NaCl, 2 mM KCl, 1 mM $MgCl_2$, 5 mM HEPES, pH 7.5 (NaOH)

4.4. Electrophysiology

4.4.1. Preparation of patch pipettes

The patch pipettes for macroscopic current measurement were fabricated from quartz tubing with an outer and inner diameter of 1.0 mm and 0.7 mm, respectively (VitroCom, New Jersey, U.S.A.). For single-channel measurements, the pipettes were fabricated from quartz tubing with an outer diameter of 1.0 mm and an inner diameter of 0.5 mm (VitroCom, New Jersey, U.S.A.). For macroscopic patches, the pipette resistance was 0.7-1.2 MΩ. For single-channel measurements, the pipette resistance was 3-10 MΩ. The cRNA-injection pipettes were pulled using a Flaming/Brown type micropipette puller (Model P-97, Sutter Instrument, Novato (CA), U.S.A.) and the macroscopic and single channel recording pipettes were pulled using a laser puller (Model P-2000, Sutter Instrument, Novato (CA), U.S.A.). Before experimental use, all pipette solutions were filtered using 0.2 µM non-pyrogenic filters (SARSTEDT AG & Co., Nümbrecht, Germany).

4.4.2. The patch-clamp technique

The patch-clamp technique allows scientists to measure the currents through ion channels in the plasma membrane. This technique was developed by Erwin Neher and Bert Sakman in the late 1970s and early 1980s to study the current flowing through single acetylcholine-activated channels in membrane patches of denervated frog muscle fibres (Neher und Sakmann 1976). In 1990, for their work on ion channels, they were awarded with the Nobel Prize in Physiology or Medicine. The patch-clamp technique permits high- resolution recording of the currents flowing through plasma membrane and is the method of choice when measuring the activity of ion channels. In our laboratory, the patch-clamp setup is composed of (1) an inverted microscope (Axiovert 100, Carl Zeiss MicroImaging GmbH, Jena, Germany) for cell visualization placed on a vibration-isolation table (Newport, Irvine (CA), U.S.A.); (2) a Faraday cage, surrounding the setup, which isolates the system from electrical noise; (3) a patch-clamp amplifier (Axopatch 200A, Axon Instruments Inc., Foster City (CA), U.S.A.) controlled by the patch-clamp software ISO2 (MFK, Niederhnhausen, Germany) on a PC; (4) a micromanipulator (Narishige, Tokyo, Japan) holding the amplifier headstage in connection with the pipette holder and the pipette; (5) a perfusion (bath) chamber; (6) a pump used for perfusion of excessive bath solution; (7) a reference electrode made of Ag/AgCl (Science Products GmbH, Hofheim, Germany) to reduce the development of a solid-liquid junction potential between the electrode and the bath solution, and (8) a recording electrode (Ag/AgCl wire) that sends the signal to the patch-clamp amplifier. In addition, we developed also a multibarrel-perfusion which allows a very fast application and removal of several ligand concentrations. In all measurements, currents were low-pass filtered at 5 kHz (4-pole Bessel). In the present study, all current recordings were made using the inside-out patch configuration with the intracellular surface of the membrane exposed to the bath solution thus, allowing a fast solution exchange at the intracellular side of the membrane (Hamill et al. 1981). Figure 4A and B show a cartoon of the patch-clamp setup and the inside-out patch clamp configuration, respectively.

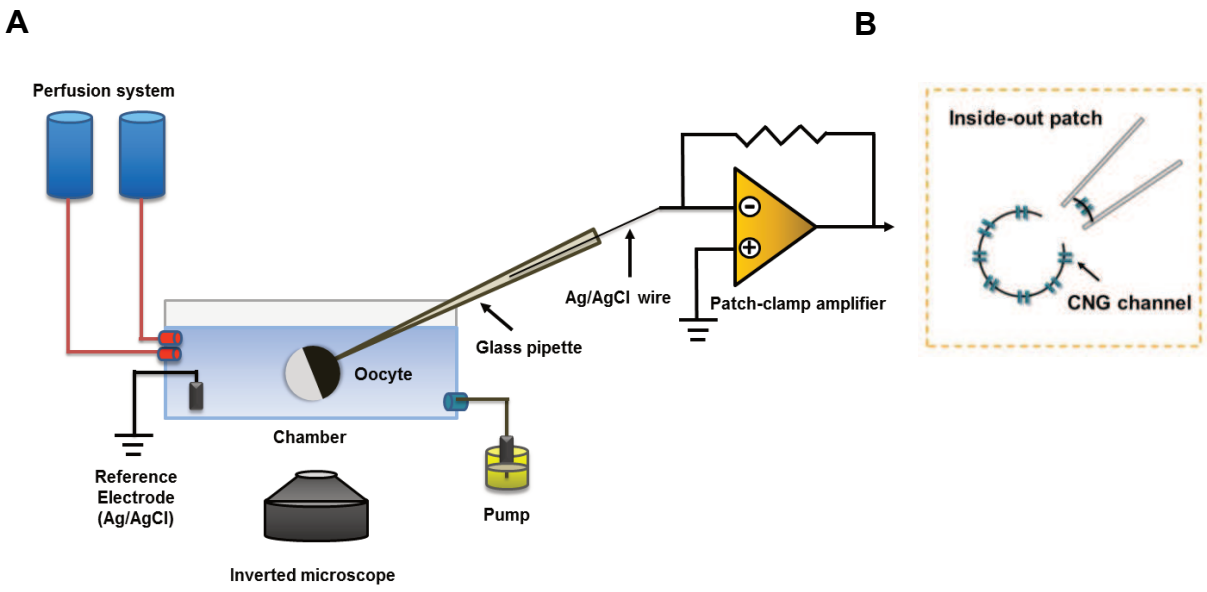

Figure 4. Cartoon showing a conventional patch-clamp setup. A) Patch-clamp setup: Before starting the experiment, the vitelline membrane of the oocytes was manually peeled. The oocytes were placed in the recording chamber, in which solutions with different ligand concentrations can be rapidly switched by a multibarrel-perfusion system. Positive pressure was applied to the pipette before immersing the patch pipette in the bath solution in order to prevent contamination of the pipette tip. B) Inside-out patch clamp: The pipette was immersed in bath solution and then attached to the oocyte membrane. When the glass pipette attached to the membrane of oocyte, the given pressure was then immediately released to obtain a giga-seal. After that the pipette was pulled away from the cell, resulting in the formation of an inside-out patch.

4.5. Data acquisition and analysis

Measurements were controlled and data were recorded with the ISO2 soft- and hardware (MFK, Niedernhausen, Germany) running on a PC. The data were analyzed by using the following software: ISO2, Microsoft Excel 2010, Origin 8G (OriginLab, Northhampton, U.S.A.).

4.5.1. Macroscopic currents

A standard experiment when studying ligand-gated ion channels is the measurement of the concentration-response relationship. This implies recording the channel response in response to different ligand concentrations. In this study, for macroscopic current measurements, electrical recordings were performed in inside-out patches and the holding voltage was 0 mV. The membrane voltage was usually stepped to -100 mV and then to +100 mV (Figure 5). The pulse duration and repetition rate of the pulses were chosen such that at the end of the pulse the current amplitude was stable. All current recordings were performed at room temperature. The currents at different cGMP concentrations were finally corrected for capacitive and very small leak currents by subtracting the respective currents measured in the absence of cGMP in the bath solution. The currents are averages of 4-12 recordings. After the inside-out patche was obtained, the patch pipette was placed in front of the first barrel of multibarrel perfusion system containing only KCl solution in order to test for possible background channel activity (leak currents) and then it was exposed to a saturating cGMP concentration to investigate the maximum current. Next, the patch pipette was exposed to solutions containing different cGMP concentrations and the respective currents were recorded. The maximum current and the leak current were measured again after the patches were exposed to at least two intermediate cGMP concentrations in order to test the patch stability or eventual changes in the saturating current.

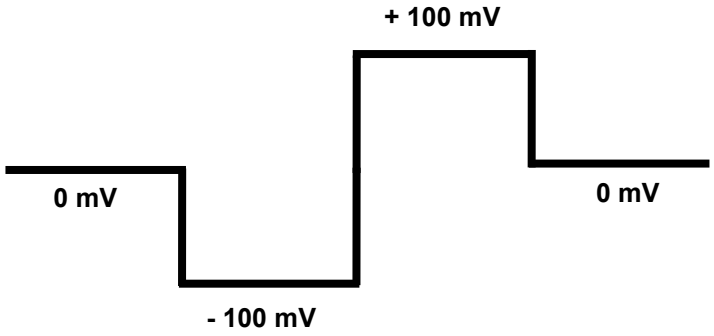

Figure 5. Pulse protocol used for macroscopic-current measurement. The holding voltage was 0 mV. The macroscopic currents in the presence of different ligand concentrations were measured first at -100 mV then at +100 mV and the window period was 1200 ms.

The concentration-response relationships were generated by relating the actual current amplitude (*I)*, to the maximum current amplitude (I_{max}) and plotting this ratio as a function of the ligand concentration (x). The data points were fitted with the Hill equation using the Origin 8G software (OriginLab, Northampton (MA), U.S.A.).

$$I/I_{max} = 1/ [1+ (EC_{50}/x)^{H}] \quad (1)$$

EC_{50} is the ligand concentration of half-maximum current and H is the Hill coefficient for channel activation. When the concentration-response relationship showed two components, the data points were fitted to the sum of two Hill equations

$$I_{max} = (1\text{-a})/[1 + (EC_{50,l}/x)^{Hl}]+ a/ [1+ (EC_{50,h}/x)^{Hh}] \quad (2)$$

where $EC_{50,l}$, $EC_{50,h}$, H_l, and H_h are the ligand concentration of half maximum current and the Hill coefficient for the low- and high-affinity component, respectively. (1 − a) and a represent the contribution of the low and high-affinity components, respectively.

4.5.2. Single-channel currents

Single-channel recordings of CNG channels were made using the inside-out patch configuration and were performed at +100 mV to achieve high amplitudes of the unitary currents. Data were filtered at a cutoff frequency of 5 kHz and sampling rate was 20 kHz. All measurements were performed at room temperature. Every patch was first exposed to KCl without cGMP to measure the leak current and then exposed to saturating and different subsaturating concentrations of cGMP All patches contained a single channel only which was confirmed by the absence of overlap-regions between two single-channel events at saturating cGMP concentration.

The analysis of single-channel recordings was performed with the ISO2 software. The distribution of all the digitized current values was plotted in a histogram. The representation of the distribution of the amplitude of events is realized in classes (bins). There was a peak at the closed level and at each of the open level(s). The area below each peak is relative to the time spent at that level. The histograms were fitted simultaneously with up to six Gaussian curves (levels) in order to examine the amplitude of the closed level and the open level(s).

The open probability (P_o) is one of the most important properties of an ion channel. It is the fraction of time the channels spends in the open state. P_o value was derived by normalized to the net current to the product of maximal current amplitude and the length of recording time. P_o varies between zero and one.

4.5.3. Global fit of concentration-response relationships from five CNGA2 concatemers

The analysis was performed in collaboration with Prof. Eckhard Schulz (Fachhochschule Schmalkalden, Schmalkalden, Germany) and Sabine Hummert (Friedrich Schiller University Jena, Jena, Germany):

Concentration-response relationships ($I/I_{max} = f([cGMP])$) of the five concatamers *wt-wt-wt-wt*, *mut-wt-wt-wt*, *mut-mut-wt-wt*, *mut-mut-mut-wt*, and *mut-mut-mut-mut* were globally fitted with the five respective models shown in Figure 17. The models are intimately coupled by common equilibrium constants. The open probability of one model is the sum of its occupation probabilities of its open states.

A Levenberg-Marquardt algorithm (Brown und Dennis 1972, Press 2002) was used to optimize the parameters of the model. The chi-square, χ^2 value was calculated from the fitted curves according to

$$\chi^2 = \sum_{i=1}^{N} \frac{(P_{o,m}(L_i) - P_{o,c}(L_i))^2}{\sigma_i^2} \quad (3)$$

$P_{o,m}$ are the normalized measured open probabilities and $P_{o,c}$ are the estimated open probabilities calculated according to Equation 3. The square of the deviations at a concentration L_i was weighted by the reciprocal squared values of the observed standard error of mean (σ_i) before adding over all N data points of all concatemers. In the fit procedure χ^2 was minimized.

4.5.4. Statistical analysis

Data are shown as mean ± SEM.

The statistical analysis was performed in collaboration with Sabine Hummert (Friedrich Schiller University Jena, Jena, Germany).

5. Results

5.1. The functional characteristics of the CNGA2 tetrameric concatemers resemble those of the channels formed by CNGA2 monomers

The concatenation technique has been used over the last years to investigate the stoichiometry and the subunit arrangement of several ion channels and receptors (Gagnon und Bezanilla 2009, Janssens und Voets 2011, White 2006). Herein, this approach was applied to the homotetrameric CNGA2 channels in order to understand those molecular processes that are triggered by the binding of the first ligand molecule. The native olfactory CNG channels form a functional heterotetrameric complex with three different subunits (2XCNGA2, 1XCNGA4 and 1XCNGB1b) (Bonigk et al. 1999, Zheng und Zagotta 2004, Bradley et al. 2001). In this work, however, we used the concatenation technique in combination with the traditional patch-clamp technique to characterize the activation of the CNGA2 homotetrameric channels because the homotetrameric channel provides a more simple model to understand channel function. To achieve this goal, the CNGA2 tetrameric concatemer was constructed by covalently linking the C-terminus of the initial CNGA2 subunit to the N-terminus of the following subunit via a short linker sequence, GSA, as described in Materials and Methods. The CNGA2 tetrameric concatemer is referred to as *wt*-*wt*-*wt*-*wt*. The electrophysiological properties of this construct were investigated and compared with those of non-concatenated CNGA2 channels in both macroscopic and single-channel recordings in order to exclude any side effects induced by this method.

5.1.1. Comparison of the concentration-response relationships obtained from CNGA2 monomers (4*wt*) and concatemers (*wt-wt-wt-wt*)

To investigate the functional properties of *wt-wt-wt-wt* channel, this construct was expressed in oocytes and the *wt-wt-wt-wt* channel activity was measured and compared with that of homotetrameric CNGA2 channels (4*wt*). All measurements were done using the inside-out patch-clamp configuration. Figure 6 shows the concentration-response relationships for the *wt-wt-wt-wt* and *4wt* channels. The currents were normalized with respect to the maximal current obtained at saturating cGMP concentration (100 µM). Both curves were fitted with Eq.1. The analysis of the concentration-response relationships showed that the cGMP concentration producing half-maximal current (EC_{50}) of both 4*wt* and *wt-wt-wt-wt* were very similar, with values of 1.92 µM and 1.97 µM, respectively. These results indicate similar cGMP apparent affinity for both constructs. The Hill coefficient (*H*) was also indistinguishable for 4*wt* and *wt-wt-wt-wt* channels with values of 2.04 and 2.27 respectively, suggesting that the degree of net positive cooperativity is not different between concatenated and non-concatenated CNGA2 subunits.

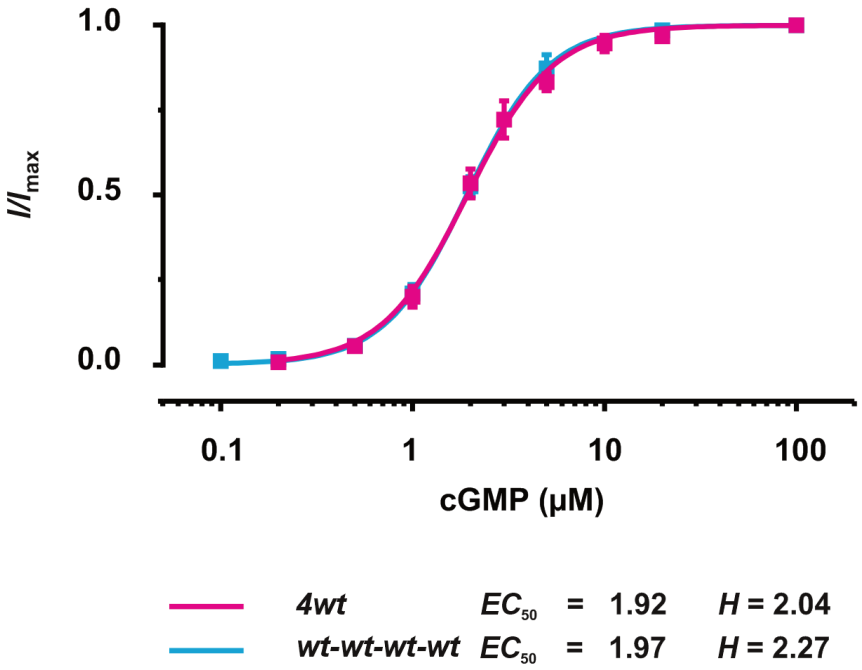

Figure 6. Concentration-response relationships of concatemeric CNGA2 channels (*wt-wt-wt-wt*, blue curve) and homotetrameric CNGA2 channels (4*wt,* pink curve) activated by various cGMP concentrations. Each point is the mean of 4 to 18 experiments. The macroscopic currents were recorded at +100 mV. The EC_{50} and Hill coefficient (*H*) values obtained from the concentration-response relationships for *wt-wt-wt-wt* and 4*wt* channels were not significantly different (Unpaired *t*-test, $p = 0.49$ for EC_{50} and $p = 0.40$ for *H*).

5.1.2. Comparison of the single-channel properties obtained from CNGA2 monomers (4*wt*) and concatemers (*wt-wt-wt-wt*)

We showed previously with macroscopic-current measurements that concatenated CNGA2 subunits were able to yield a functional channel and its concentration-response relationship was not different from that of a channel formed by monomers. We extensively compared the single-channel properties including single-channel current amplitude (*i*) and open probability (P_o) obtained from 4*wt* channels with those obtained from *wt-wt-wt-wt* channels to further ensure that the concatenation technique does not influence channel function at the single-channel

level. The 4*wt* and *wt-wt-wt-wt* currents were investigated in single-channel patches after the channels were fully activated by saturating cGMP concentrations of 100 µM. Three representative traces for each construct are shown in Figure 7A. The open probability of the *wt-wt-wt-wt* channels (P_o = 0.99 ± 0.002) was identical to that of 4*wt* channels (P_o = 0.99 ± 0.002). Figure 7B presents the amplitude histograms for the two constructs in the presence of saturating cGMP concentration. For 4*wt* the obtained single-channel amplitude (*i*) was 4.99 ± 0.43 pA and for *wt-wt-wt-wt was* 5.11 ± 0.24 pA. The concatemeric construct gave rise to currents with only one conductance level. No subconductance events could be observed. These findings resemble very closely the characteristics of 4*wt* channels. The values of single-channel properties are summarized in Table 1.

Based on our findings from the macroscopic and single-channel data regarding the EC_{50}, *H*, current amplitude and open probability for the CNGA2 concatenated and non-concatenated channels, we conclude that the concatenation technique does not influence the channel function.

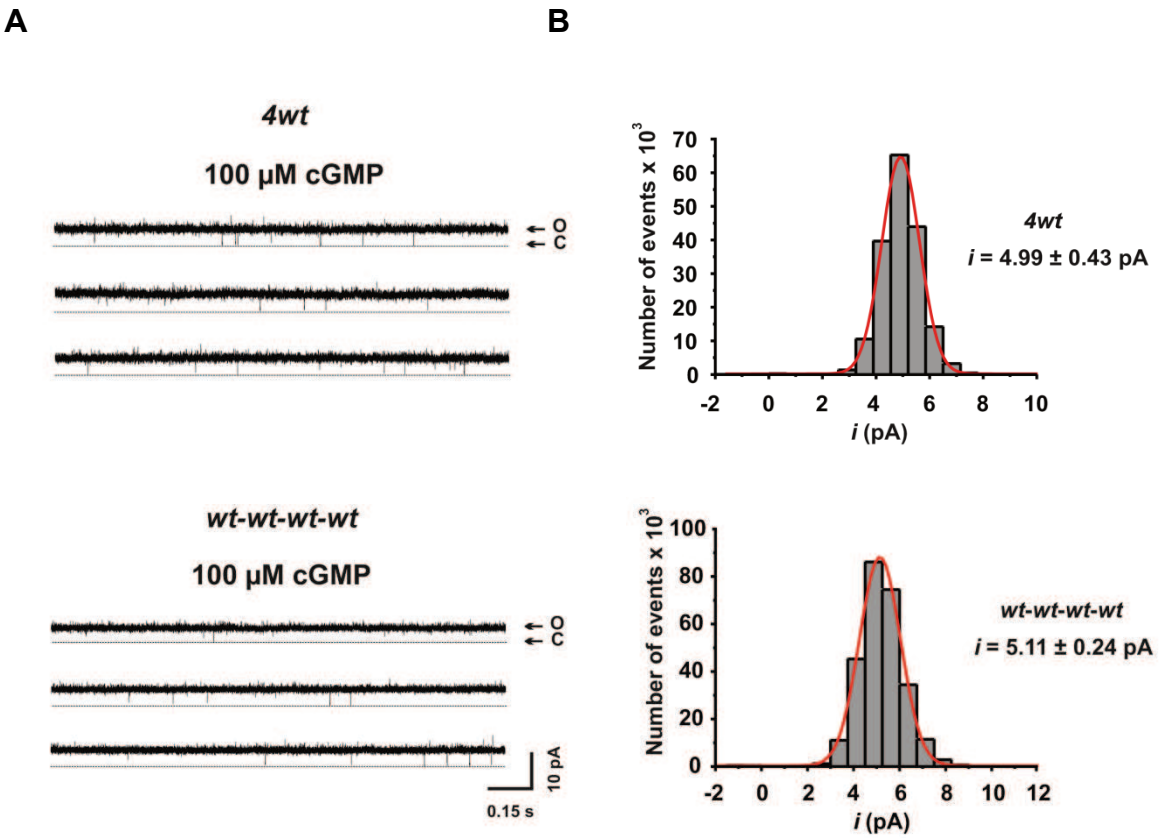

Figure 7. Single-channel properties of 4*wt* and *wt-wt-wt-wt* channels. A) Representative single-channel traces of 4*wt* and *wt-wt-wt-wt* channels recorded in the presence of saturating cGMP concentration. The data were recorded with the membrane voltage clamped at +100 mV. The channel opening for all constructs was close to 100 % with only brief channel closures. No flickering activity or subconductance levels were observed. The current levels of open channel (o) and closed channel (c) were indicated by arrows. B) All points current amplitude histograms of 4*wt* and *wt-wt-wt-wt* channels at saturating cGMP concentration. Single-channel current amplitudes (*i*) were obtained after fitting the data with the sum of two Gaussian functions. The amplitudes of the single-channel current and the P_o of the two constructs were not significantly different (Unpaired *t*-test, p = 0.81 for i and p = 0.61 for P_o).

Table 1. Open probability and single-channel current amplitude for 4*wt* and *wt-wt-wt-wt* channels at saturating cGMP concentration

Constructs	cGMP (μM)	*i* (pA)	P_o	*N*
4wt	100	4.99 ± 0.43	0.99 ± 0.002	4
wt-wt-wt-wt	100	5.11 ± 0.24	0.99 ± 0.002	4

Parameters are shown as mean ± SEM values. *i* is the current amplitude. P_o is the open probability. *N* is the number of experiments.

5.1.3. Single-channel properties of *wt-wt-wt-wt* channels at different ligand concentrations

The functional characteristics of the CNGA2 concatemers were further investigated at the single-channel level. The reasons for the measurement of single-channel activity were 1) to assess the detailed characteristics of concatemeric CNGA2 channels properties without the influence of oocytes endogenous channel activity and 2) to further ensure that the covalent linkage does not affect channel function at the single-channel level. The single-channel properties of *wt-wt-wt-wt* channel, including single-channel current amplitude (*i*) and open probability (P_o) were examined at various subsaturating cGMP concentrations. The oocytes were injected with the respective cRNA and one or two days after injection the measurements were performed. Single-channel currents were recorded under steady-state conditions at +100 mV after activation by 0 μM (without ligand), 1 μM, 3 μM, 10 μM, 25 μM and 100 μM cGMP (saturating concentration).

Figure 8 presents three representative single-channel current traces at the respective cGMP concentrations. At all cGMP concentrations tested the channels opened to a single and stable conductance level (e.g., no bursting behavior and no

subconductance levels were observed). In the absence of the ligand, the channels could open spontaneously with a very low open probability ($P_o = 4x10^{-4} \pm 2.4x10^{-4}$). These results are consistent with several previous reports on multichannel patches suggesting that in the absence of cyclic nucleotides, the CNG channels can open spontaneously with very low probability (Li and Lester 1999, Tibbs et al. 1997, Picones and Korenbrot 1995). The open probability increased with increasing cGMP concentrations (1 µM: $P_o = 0.22 \pm 0.14$; 3 µM: $P_o = 0.76 \pm 0.08$; 10 µM: $P_o = 0.98 \pm 0.009$; 25 µM: $P_o = 0.99 \pm 0.004$). Also, the single-channel current amplitudes were measured at all cGMP concentrations tested. Precise single-channel current amplitudes were estimated from the all-point histograms of each measurement and the peaks of the closed level were used to subtract leak currents. The number of events obtained in each bin was normalized to the total number of events observed. The amplitude histograms for each measurement were normalized to unit area and the data were fitted by sums of two Gaussian functions, yielding the corresponding mean values of single-channel current amplitudes (i) as follows: 1 µM: $i = 4.77 \pm 0.11$ pA; 3 µM: $i = 4.85 \pm 0.13$ pA; 10 µM: $i = 4.91 \pm 0.15$ pA; 25 µM: $i = 4.55 \pm 0.20$ pA; 100 µM: $i = 5.11 \pm 0.24$ pA). Figure 9 shows the representatives amplitude histograms for each cGMP concentration. These results clearly show that the amplitudes of the single-channel current of concatemeric CNGA2 channels did not depend on the cGMP concentrations as also observed for the CNGA2 (4*wt*) channels (from Eberhard M. unpublished data). The herein determined single-channel parameters are summarized in Table 2.

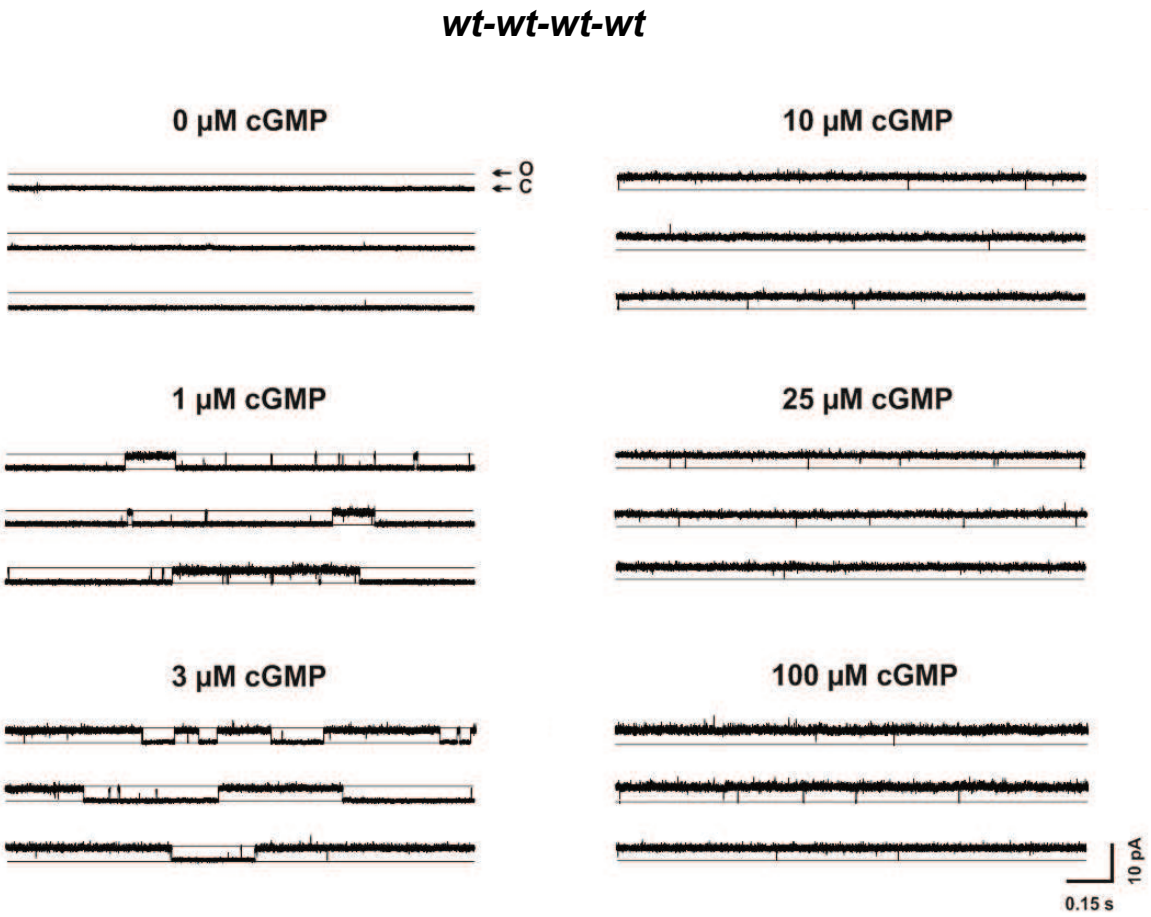

Figure 8. Representative single-channel traces of *wt-wt-wt-wt* CNGA2 channels. The single-channel activity was recorded at 0 µM, 1 µM, 3 µM, 10 µM, 25 µM and 100 µM (*N* = 4-6) with the membrane voltage clamped at +100 mV. At 0 µM, the channel could open with very low open probability. The open probability decreases as the cGMP concentration decreases. Neither flickering behavior nor subconductance levels were observed. The current levels of open channel (o) and closed channel level (c) are indicated by arrows.

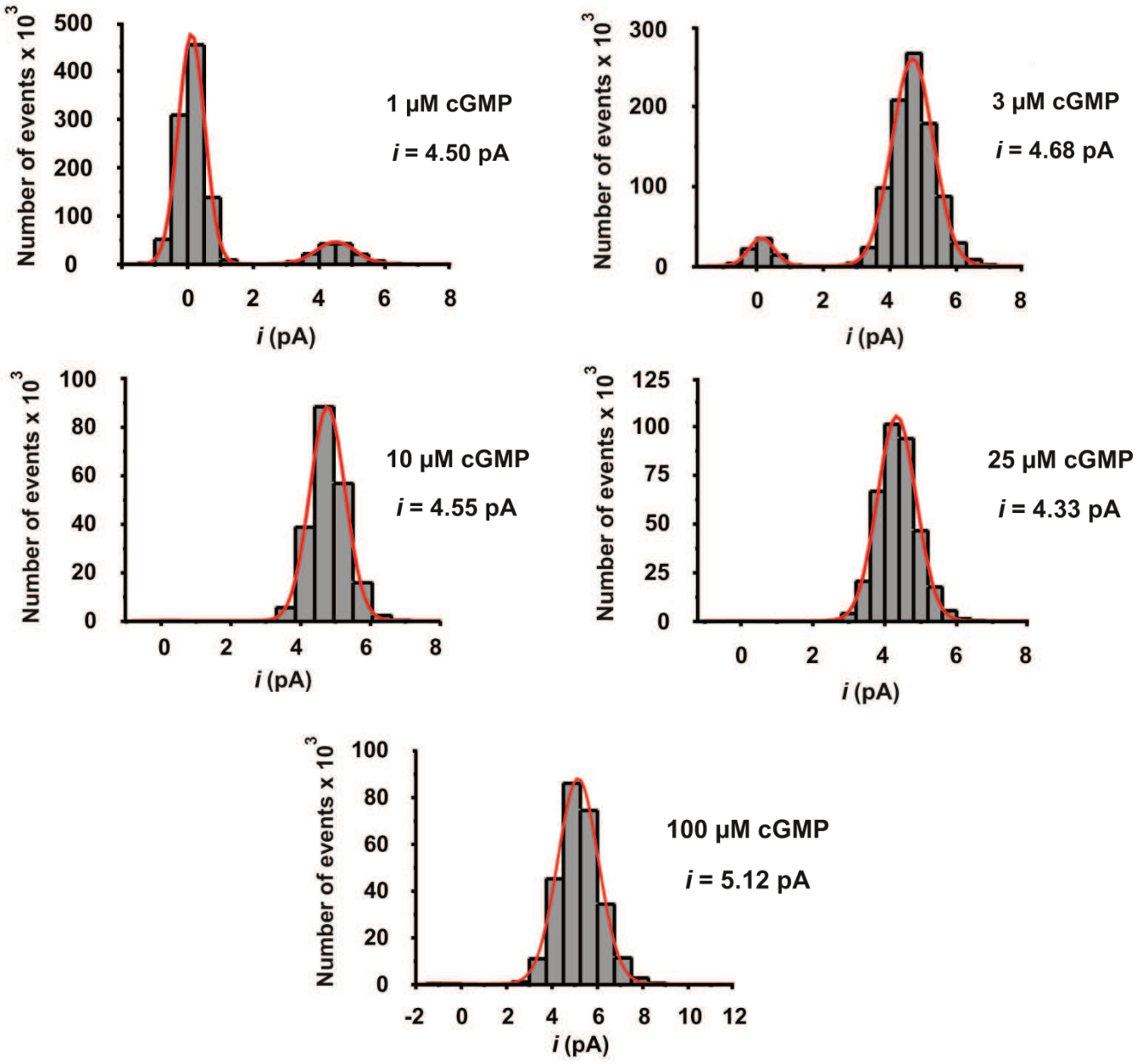

Figure 9. All points amplitude histograms of *wt-wt-wt-wt* CNGA2 channels at different cGMP concentrations. The amplitudes of the single-channel current (*i*) were obtained after fitting the data with the sum of two Gaussian functions. The amplitudes of the single-channel current at all cGMP concentrations tested are not significantly different (One-way ANOVA, $p = 0.29$) suggesting that the single-channel amplitude does not depend on the cGMP concentration. The values of single channel current amplitudes (*i*) obtained at the respective cGMP concentrations are shown in the right-upper panels.

Table 2. Open probability and single-channel current amplitude for *wt-wt-wt-wt* channels at different cGMP concentrations

cGMP (μM)	*i* (pA)	P_o	*N*
0	-	$4.0x10^{-4} \pm 2.4x10^{-4}$	5
1	4.77 ± 0.11	0.22 ± 0.14	4
3	4.85 ± 0.13	0.76 ± 0.08	4
10	4.91 ± 0.15	0.98 ± 0.009	5
25	4.55 ± 0.20	0.99 ± 0.004	4
100	5.11 ± 0.24	0.99 ± 0.002	4

Parameters are shown as mean ± SEM values. *i* is the current amplitude. P_o is the open probability. *N* is the number of experiments.

5.2. The concatenated CNGA2 channels have the expected subunit arrangement

We had to make sure that the subunits are still linked after the concatemers were injected into oocytes and the enzymes did not digest the inserted linkers between subunits. Hence, control experiments were mandatory to confirm the proper incorporation of *wt-wt-wt-wt* channels in the plasma membrane with the correct complement of subunits. The control experiments relied on a mutated CNGA2 (R538E) subunit as a reporter mutation. A previous report showed that the CNGA2 channel formed by CNGA2 (R538E) subunits exhibited a decreased apparent

affinity for cGMP with the EC_{50} value of 606.7 µM (Nache et al. 2012). This means that the binding site mutation reduces the ligand sensitivity of the channel by a factor of ~300. A straightforward way to validate the intact concatemeric CNGA2 construct was to compare the concentration-response relationships of 4*wt* and *wt-wt-wt-wt* with that of *wt-wt-wt-wt* channels coexpressed with CNGA2 with mutated binding site (R538E, *mut* subunits). Our expectation was that if the *wt-wt-wt-wt* construct was intact, the concentration-response relationship obtained from coexpressing *wt-wt-wt-wt* with a *mut* monomer should be identical to that obtained from the *wt-wt-wt-wt* construct alone. In this experiment, we used cAMP as an agonist because when coexpressing CNGA2 subunits with modulatory subunits, for examples CNGA2+CNGA4, CNGA2+CNGB1b and CNGA2+CNGA4+CNGB1b, the shift of the concentration-response relationships of these heterotetrameric channels along the cAMP-concentration axis was much bigger than those with cGMP and therefore easier to distinguish between the respective channels (Nache et al. 2013). The cRNAs encoding for either 4*wt*, *wt-wt-wt-wt* or *wt-wt-wt-wt* channels were coexpressed with that of CNGA2 (R538E) monomer (*mut*). After 3-4 days of cRNAs injection, the concentration-response relationships of the three constructs were measured. All curves were best fits with Eq. 1.

Figure 10 shows that the concentration-response relationship obtained from *wt-wt-wt-wt* + *mut* was very similar to both, 4*wt* and *wt-wt-wt-wt* channels, regarding the apparent affinity to cAMP and Hill coefficients. For 4*wt*, EC_{50} = 59.01 µM, H = 2.22; for *wt-wt-wt-wt*, EC_{50} = 56.17 µM, H = 1.90 and for *wt-wt-wt-wt* + *mut*, EC_{50} = 61.24 µM, H = 2.15. These results confirm our previous findings (see 4.1.) that the concatenation technique does not have any side-effects on the CNGA2 channel function. In conclusion, the *wt-wt-wt-wt* concatemers are intact and indeed assemble as tetrameric channels. The performed control macroscopic and single-channel experiments strongly suggest that the concatenation technique is a proper approach for studying gating effects of individual subunits.

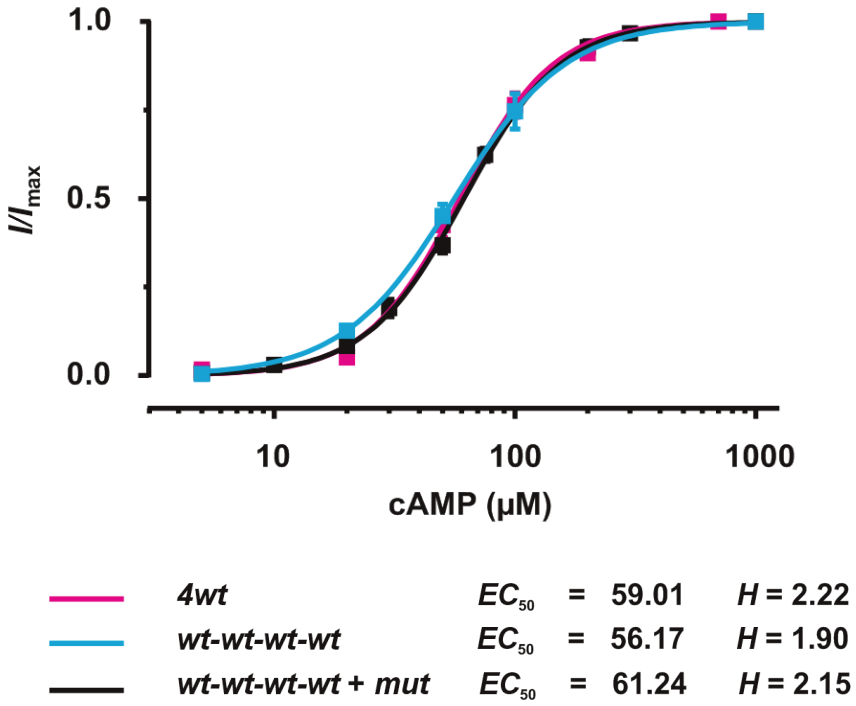

Figure 10. Concentration-response relationships of homotetrameric CNGA2 channels (*4wt*), concatemeric CNGA2 channels (*wt-wt-wt-wt*) and *wt-wt-wt-wt* coexpressed with CNGA2 (R538E) monomers (*wt-wt-wt-wt* + *mut*). Each point is the mean of 4 to 15 experiments at +100 mV. The EC_{50} and Hill coefficient (*H*) obtained from all constructs were not significantly different (One-way ANOVA, p = 0.27 for EC_{50} and p = 0.40 for *H*). No shift in the resulting concentration-response relationship was observed when coexpressing the concatemers with *mut* monomers indicating that the *mut* monomers were not incorporated into the channels.

5.3. Functional characterization of CNGA2 tetrameric concatemers containing varying numbers of functional binding domains

After we confirmed that the concatenation technique can be successfully applied to study CNGA2 channels, we then considered to construct and electrophysiologically characterize CNGA2 tetrameric concatemers containing different numbers of functional binding domains. The concatenation technique allowed us to control the number and the position of the mutated subunits in the respective constructs. Our aim was to describe the contribution of each individual subunit to the activation of the homotetrameric CNGA2 channels. By means of a point mutation in the cyclic nucleotide binding site (R538E), concatemers were constructed containing 1, 2, 3 or 4 disabled subunits (*mut-wt-wt-wt*, *mut-mut-wt-wt*, *mut-mut-mut-wt* and *mut-mut-mut-mut*). The respective concentration-response relationships obtained from macroscopic-current measurements are shown in Figure 11. The concentration-response relationships for the four concatemers were progressively shifted to higher cGMP concentrations in proportion to the number of *mut* subunits. A systematic decrease of the Hill coefficient (*H*) was also observed for all constructs, except for that of the *mut-mut-mut-mut* channel which was quite similar to that of the *wt-wt-wt-wt* channel.

For the respective channels that are either formed by four monomers (4*wt*, 4*mut*) or by tetrameric concatemers (*wt-wt-wt-wt*, *mut-wt-wt-wt*, *mut-mut-wt-wt*, *mut-mut-mut-mut*), all concentration-response relationships were successfully fitted by one component fits (Eq. 1), yielding: for 4*wt*: EC_{50} = 1.92, H = 2.04; for 4*mut*: EC_{50} = 606.67, H = 2.65; for *wt-wt-wt-wt*: EC_{50} =1.97, H = 2.27; for *mut-wt-wt-wt*: EC_{50} = 2.87, H = 1.44; for *mut-mut-wt-wt*: EC_{50} = 6.79, H = 1.30; for *mut-mut-mut-mut*: EC_{50} = 687.7, H = 2.35. Interestingly, the concentration-response relationship obtained from *mut-mut-mut-wt* required the sum of two Hill functions (Eq. 2), indicating the presence of two components: a high and a low affinity component. The fit characterizing the *wt* subunit and the mutated subunits, respectively, yielded: $EC_{50,h}$ = 44.34, H_h = 1.0 (fixed), $EC_{50,l}$ = 354.12, H_l = 2.15, a = 0.63 (a is the contribution of the low affinity component to channel activation).

For a better visualization of the effects of the progressive loss of CNGA2 functional binding domains on channel function, we next plotted the relationships of either EC_{50} or Hill coefficients (H) (Figure 12) with respect to the number of functional subunits. Figure 12A shows that the EC_{50} systemically decreases when the number of functional subunits increases. The most noticeable shift in the EC_{50} toward smaller ligand concentrations was generated by the recruitment of the second functional subunit, followed by smaller effects with each additional functional subunit. The apparent affinity increased by 37.55 μM with the second functional subunit, whereas the presence of the third and the fourth functional subunits increased the apparent affinity of the channel only by 3.92 and 0.9 μM, respectively.

The corresponding Hill coefficient (H) reached a maximum when the channels contained all four functional binding domains (Figure 12B), suggesting a graded increase in the cooperativity between subunits with increasing number of functional binding sites.

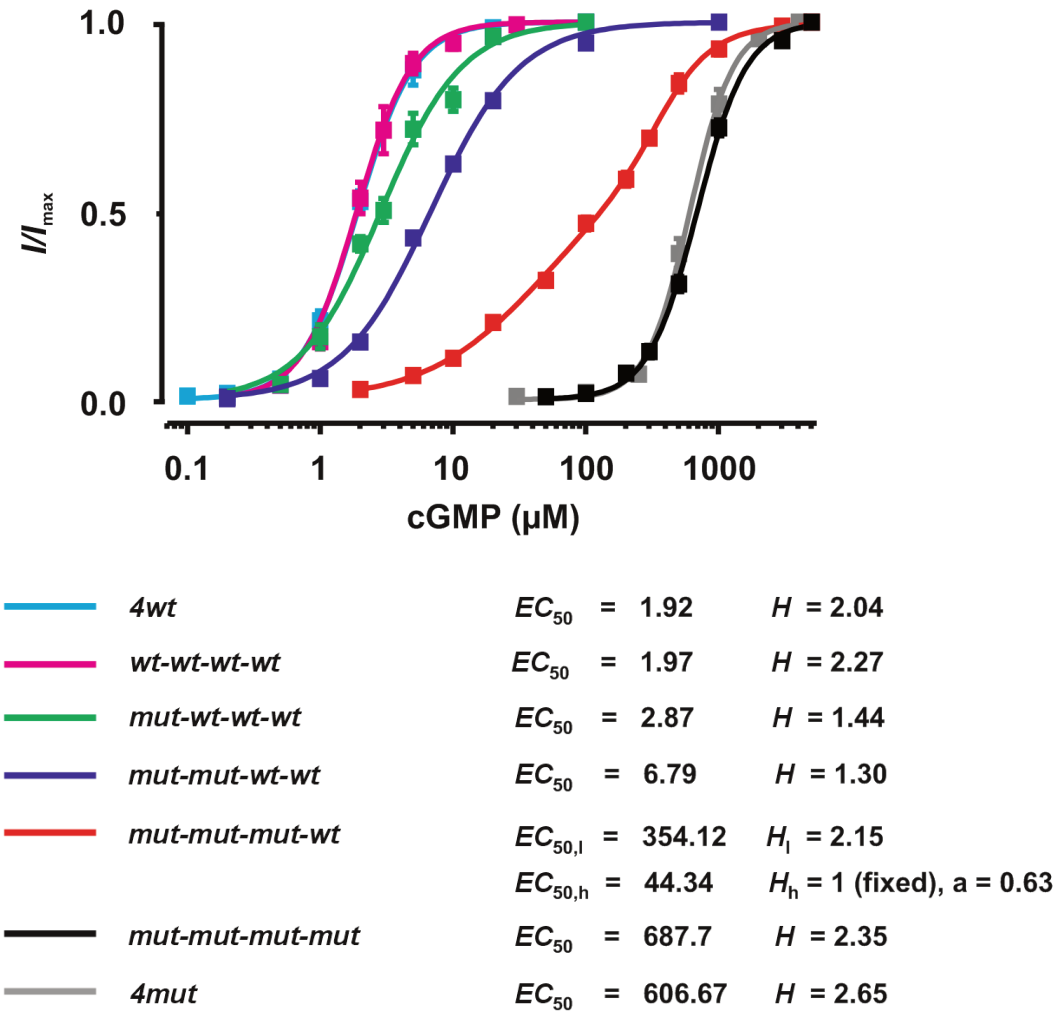

Figure 11. Concentration-response relationships for macroscopic currents induced by different cGMP concentrations in CNGA2 tetrameric concatemers containing 0, 1, 2, 3 or 4 disabled subunits: *wt-wt-wt-wt* (pick curve), *mut-wt-wt-wt* (green curve), *mut-mut-wt-wt* (purple curve), *mut-mut-mut-wt* (red curve), *mut-mut-mut-mut* (black curve) and in homotetrameric CNGA2 wild-type (4*wt*, blue curve) and homotetrameric CNGA2(R538E) mutants (4*mut*, grey curve). Each point is the mean of 4 to 15 experiments at +100 mV. The concatemers containing 1, 2, 3, or 4 disabled subunits showed a progressive loss of the cGMP sensitivity (EC_{50}). A systematic decrease of the Hill coefficient (*H*) was also observed for all constructs, except that *H* for *mut-mut-mut-mut* was indistinguishable to that of *wt-wt-wt-wt*. All curves, except *mut-mut-mut-wt* were successfully fitted with one component fits (Eq. 1). In contrast, *mut-mut-mut-wt* was fitted with two components (Eq. 2), indicating that this construct contains two functional components: a high and a low cGMP affinity component.

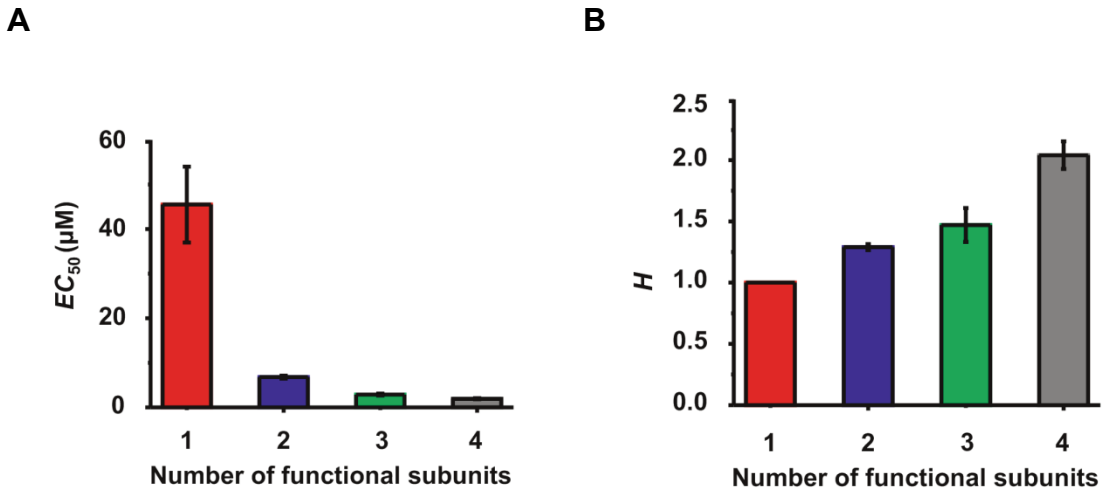

Figure 12. Changes in EC_{50} and Hill coefficient (H) with the number of functional CNGA2 subunits. A) The relationship between the EC_{50} and the number of functional subunits is not linear. A strong increase in the apparent affinity is generated by the recruitment of the second functional subunit, whereas the presence of the third and the fourth functional binding sites determines much smaller effects. B) The corresponding Hill coefficient is maximal when all four subunits actively participate by ligand binding to channel opening.

5.4. The position of the functional subunit(s) in a CNGA2 concatemer is of minor importance for the channel function

Next, we addressed the question whether the position of functional subunit(s) has any effect on the channel function. Also, by changing the position of the *wt*-subunit(s) in the channel eventual intersubunit interaction could be identified. We therefore compared the functional characteristics of all concatemers containing one functional subunit occupying different positions in the channel: *mut-mut-mut-wt*, *mut-wt-mut-mut, mut-mut-wt-mut, wt-mut-mut-mut*. The same strategy was also applied for concatemers with two functional subunits located in either *trans* configuration (*wt-mut-wt-mut* and *mut-wt-mut-wt*) or *cis* configuration (*mut-mut-wt-wt* and *wt-wt-mut-mut*). These constructs were expressed in oocytes and the

functional characteristics of the respective channels were evaluated in inside-out macroscopic patches.

For all constructs with only one functional binding site (Figure 13A), the respective concentration-response relationships were well fitted by a sum of two Hill equations (Eq. 2), yielding: for *mut-mut-mut-wt*: $EC_{50,h}$ = 44.34, H_h = 1.0 (fixed), $EC_{50,l}$ = 354.12, H_l = 2.26, a = 0.63; for *mut-wt-mut-mut*: $EC_{50,h}$ = 80.90, H_h = 1.0 (fixed), $EC_{50,l}$ = 352.0, H_l = 2.63, a = 0.88; for *mut-mut-wt-mut*: $EC_{50,h}$ = 49.61, H_h = 1.0 (fixed), $EC_{50,l}$ = 251.5, H_l = 1.48, a = 0.51; and for *wt-mut-mut-mut*: $EC_{50,h}$ = 20.43, H_h = 1.0 (fixed), $EC_{50,l}$ = 163.16, H_l = 1.50, a = 0.29 (a is the contribution of the low affinity component to channel activation).

For the constructs with two functional binding sites (Figure 13B), the concentration-response relationships were well fitted by one Hill equation (Eq. 1), yielding: for *mut-mut-wt-wt*: EC_{50} = 6.79, H = 1.30; for *wt-mut-wt-mut*; EC_{50} = 8.76, H = 1.20; for *mut-wt-mut-wt*; EC_{50} = 8.61, H = 1.34; and for *wt-wt-mut-mut*; EC_{50} =7.74, H = 1.31. Both graphs show that although the position of the functional subunit(s) in each construct was different, the concentration-response relationships for the concatemers containing one functional subunit were not statistically different as were the concentration-response relationships for the concatemers containing two functional subunits (multidimensional *t*-test with Holm correction, p=1). This suggests that changing the position of the functional subunit(s) in the channel does not lead to arrangement specific changes of the functional characteristics of the channel. It is only the number of binding steps which has a greater impact on the channel behaviour but not the interaction with the neighbouring subunits.

A

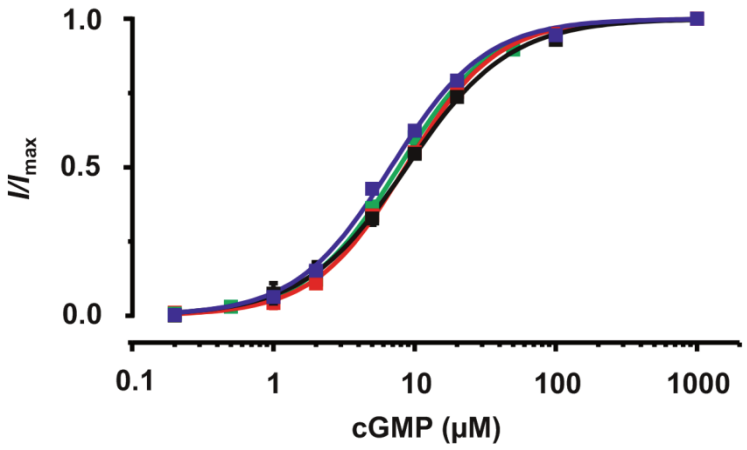

mut-mut-mut-wt	$EC_{50,l}$ = 354.12	H_l = 2.26	$EC_{50,h}$ = 44.34	H_h = 1	a = 0.63
mut-wt-mut-mut	$EC_{50,l}$ = 352.0	H_l = 2.63	$EC_{50,h}$ = 80.90	H_h = 1	a = 0.88
mut-mut-wt-mut	$EC_{50,l}$ = 251.50	H_l = 1.48	$EC_{50,h}$ = 49.61	H_h = 1	a = 0.51
wt-mut-mut-mut	$EC_{50,l}$ = 163.16	H_l = 1.50	$EC_{50,h}$ = 20.43	H_h = 1	a = 0.29

B

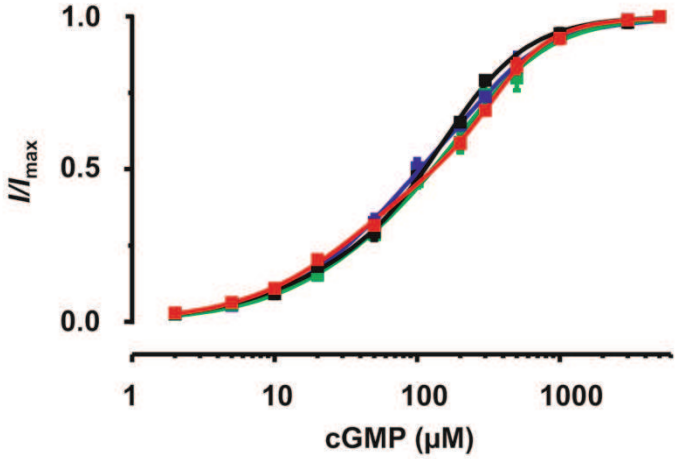

mut-mut-wt-wt	EC_{50} = 6.79	H = 1.30
wt-mut-wt-mut	EC_{50} = 8.76	H = 1.20
mut-wt-mut-wt	EC_{50} = 8.61	H = 1.34
wt-wt-mut-mut	EC_{50} = 7.74	H = 1.31

Figure 13. The position of functional subunit(s) in the concatemeric channels is less relevant for the channel function. A) Concentration-response relationships for concatemers containing two functional subunits located at different positions within the channel. The colored curves represent as follows: *mut-mut-wt-wt* (blue curve), *wt-mut-wt-mut* (black curve), *mut-wt-mut-wt* (red curve) and *wt-wt-mut-mut* (green curve). B) Concentration-response relationships for concatemers containing only one functional subunit located at different positions within the channel. The colored curves represent as follows: *mut-mut-mut-wt*, red curve; *mut-wt-mut-mut*, blue curve; *mut-mut-wt-mut*, green curve; *wt-mut-mut-mut*, black curve. The curves for concatemers with one functional subunit were indistinguishable as were the curves for the constructs with two functional subunits (multidimension *t*-test with Holm correction, $p=1$) indicating that it is the number but not the position of functional subunit(s) that has a greater effect on the channel behavior.

5.5. Characterization of CNGA2 channel activation induced by the first ligand binding step

Despite the growing insight into the ligand binding and CNG channel activation, it still remains of fundamental interest to study the work of a single subunit embedded in a working channel. Therefore, the main objective of this work was to characterize the CNGA2 activation after the first ligand binding step. In this part we sought to determine the contribution of an individual CNGA2 subunit to channel function in *mut-mut-mut-wt* channel. Therefore, not only single-channel measurements but also macroscopic-current measurements were performed.

5.5.1 Single-channel analysis of CNGA2 channel activation induced by the first ligand binding step

We first began by characterizing the single-channel properties of the concatemeric CNGA2 channel containing only one functional subunit. We got an estimate of the single-channel current amplitudes and open probability obtained from the *mut-mut-mut-wt* construct by using the inside-out patch configuration under steady-state conditions at +100 mV. The single-channel patches were exposed to different

cGMP concentrations as follows: 0 µM, 1 µM, 3 µM, 10 µM, 20 µM and 3000 µM, respectively. These concentrations were selected using the concentration-response relationship obtained from macroscopic patches of the respective channel (see 4.3.). We assumed that in the lower concentration range only the functional binding site is occupied, whereas in the higher concentration range the binding takes place mainly to the mutated subunits. Three representative traces for each cGMP concentration tested are shown in Figure 14. The channel opened spontaneously in the absence of cGMP binding (P_o = 1.7x10^{-5} ± 1.0x10^{-6}). At saturating concentration, 3000 µM cGMP, the probability of opening approached unity (P_o = 0.99 ± 0.005) and the open state was interrupted only by very brief closures. The obtained open probabilities were: 1 µM: P_o = 0.005 ± 0.001; 3 µM: P_o = 0.03 ± 0.008; 10 µM: P_o = 0.10 ± 0.02; 20 µM: P_o = 0.20 ± 0.05. Interestingly, the first binding step already induced the full channel opening and no subconductance levels could be seen.

To determine single-channel current amplitudes at different cGMP concentrations, the amplitude histograms for each measurement were analyzed and fitted to the sum of two Gaussian functions, yielding the following mean values: 1 µM: i = 4.86 ± 0.51 pA; 3 µM: i = 4.70 ± 0.13 pA; 10 µM: i = 4.67 ± 0.14 pA; 20 µM: i = 4.58 ± 0.11 pA; 3000 µM: i = 4.78 ± 0.17 pA. Figure 15 shows the representatives of the amplitude histograms for each cGMP concentration.

In summary, we were able to show that already the first binding step fully opens the channel reaching the full conductance level. The next binding steps lead only to changes in the open probability of the channel. The herein determined single-channel parameters are summarized in Table 3.

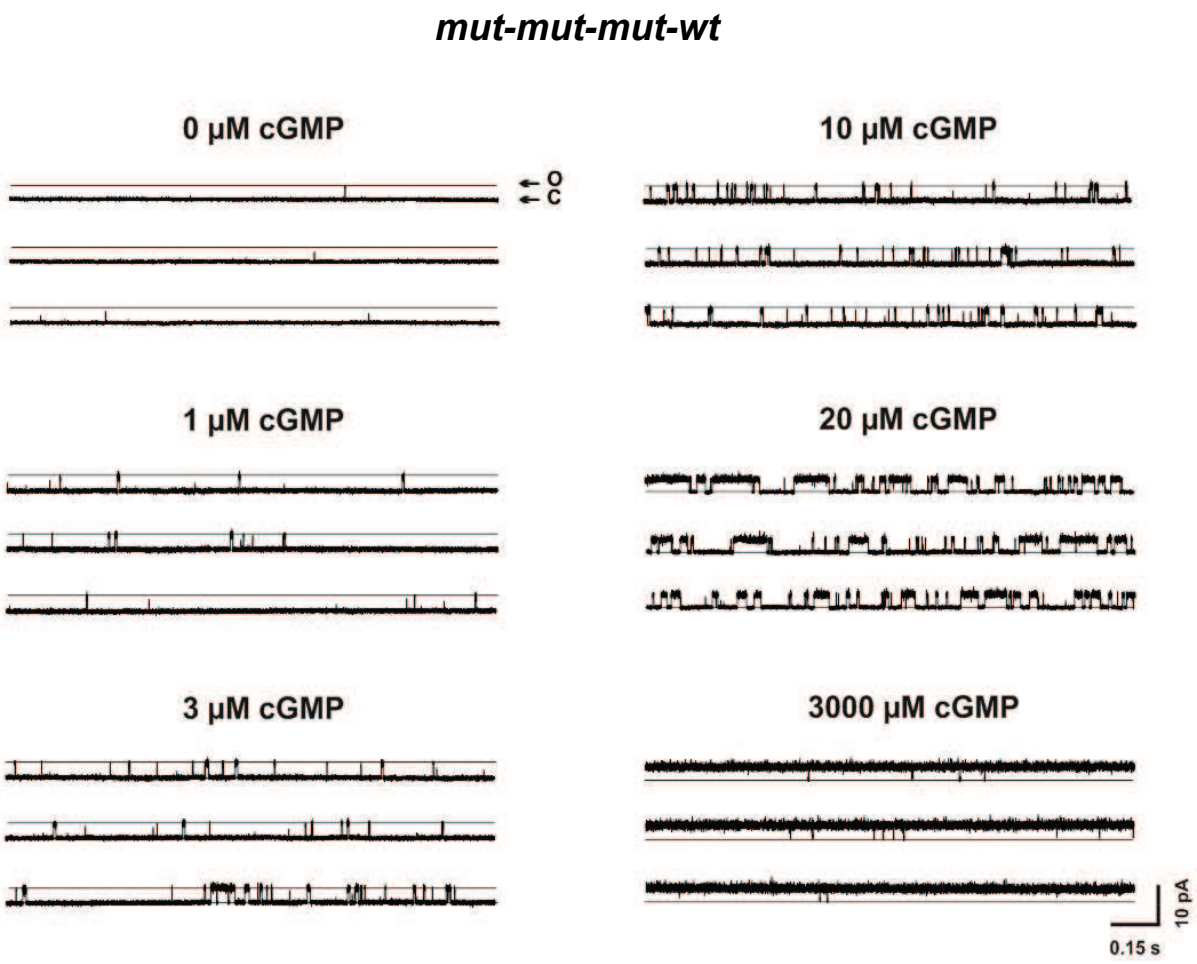

Figure 14. Representative single channel traces of *mut-mut-mut-wt* channel at different cGMP concentrations. The membrane voltage was clamped at +100 mV. The patches were exposed to 0, 1, 3, 10, 20 and 3000 µM cGMP. At 3000 µM, not only the *wt* subunit but also the *mut* subunits were activated. However, we assume that at cGMP concentrations lower than 10 µM only the functional subunit was activated (see also Figure 17). The single-channel currents show only one conductance state indicating that despite the fact that the tetrameric concatemer contains only one functional subunit, this activated subunit can trigger full channel opening. The current levels of open channel (o) and closed channel level (c) are indicated by arrows.

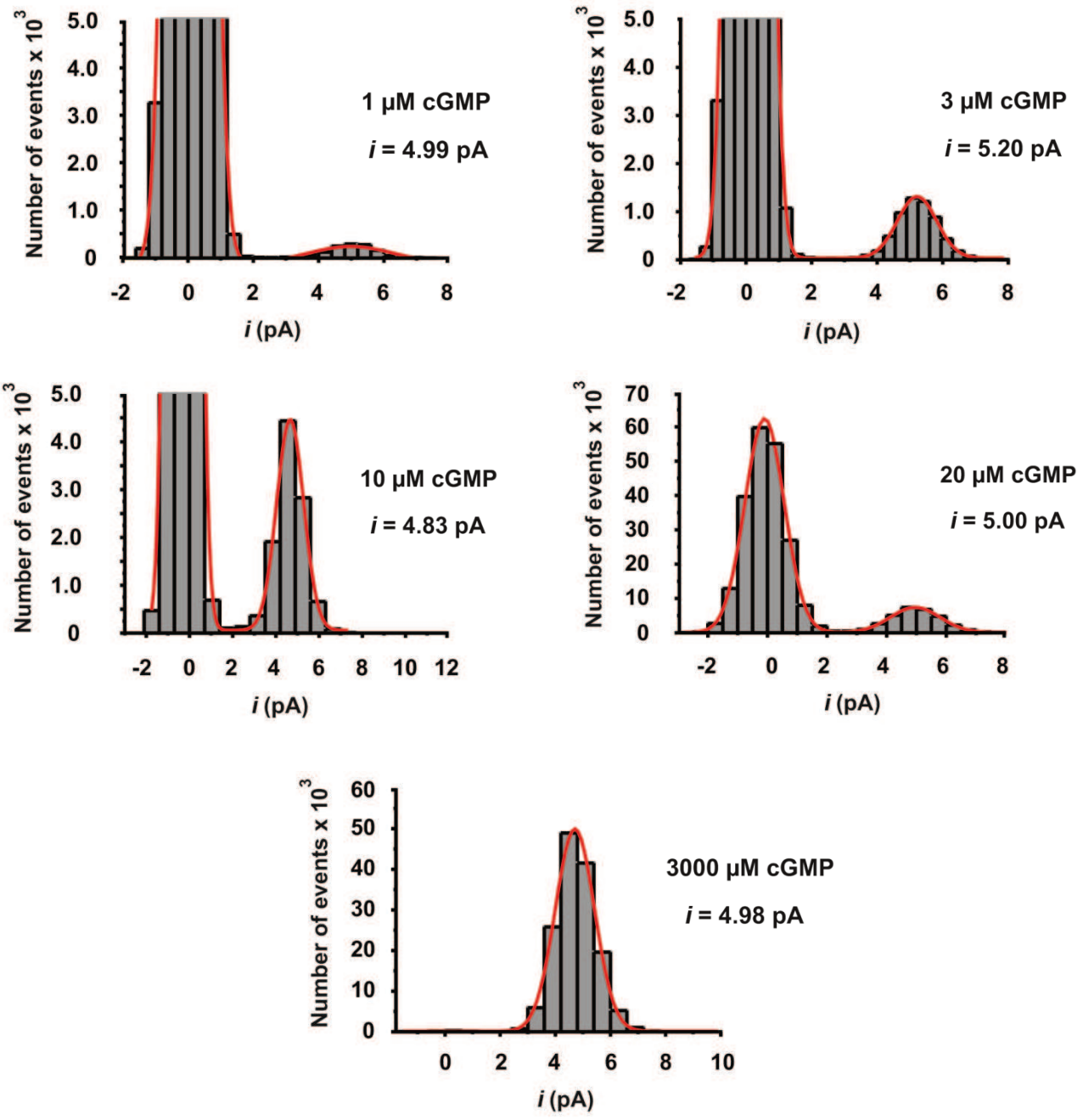

Figure 15. All points amplitude histograms of *mut-mut-mut-wt* channel at different cGMP concentrations. The values of single-channel current amplitudes and the respective cGMP concentration are indicated in right-upper panels. The representative amplitudes of the single-channel current at the indicated cGMP concentrations are not significantly different (One-way ANOVA, p = 0.89) suggesting that the amplitudes of the single-channel current do not depend on the cGMP concentration.

Table 3. Open probability and single-channel current amplitude for *mut-mut-mut-wt* channels at different cGMP concentrations

cGMP (μM)	*i* (pA)	P_o	*N*
0	-	$1.7x10^{-5} \pm 1x10^{-6}$	4
1	4.86 ± 0.51	0.005 ± 0.001	4
3	4.70 ± 0.13	0.03 ± 0.008	8
10	4.67 ± 0.14	0.10 ± 0.02	8
20	4.58 ± 0.11	0.20 ± 0.05	8
3000	4.78 ± 0.17	0.99 ± 0.005	4

Parameters are shown as mean ± SEM values. *i* is the current amplitude. P_o is the open probability. *N* is the number of experiments.

5.5.2. Characterization of channel activation induced by the first binding step in multichannel patches

We have learned from previous experiments (see 4.3.) that a selective loss of CNGA2 functional binding domains leads to a graded decrease of channel apparent affinity. Apart from *mut-mut-mut-wt* construct, all concentration-response relationships were well described by one Hill function (Eq. 1) suggesting that the activation of the channel is triggered mainly by the ligand binding to the *wt* subunits only and the contribution of the *mut* subunits is only minor. For the *mut-mut-mut-wt* construct, two components were identified in the concentration-response

relationship. The first component describes the functional characteristics of the mutated CNGA2 subunit (*mut*) with lower cGMP sensitivity and the high-affinity component characterizes the functional CNGA2 (*wt*). Figure 16 shows the P_o values plotted with respect to the cGMP concentrations for the respective constructs. We observed from the fit that the channel reaches already after the first binding step approximately 63% of its maximal open probability. We next selected representative P_o values (see 4.5.1.) at 3 µM, 10 µM and 20 µM cGMP from single-channel data and compared them with P_o values from macroscopic measurements (see right insert in Figure 16). As expected, the results showed that the open probabilities obtained from macroscopic measurements were very similar to those values obtained from existing single-channel recordings.

Nevertheless, caution is required when considering the contribution of the first activated subunit as this finding could be contaminated by the binding of the second subunit. Therefore, the next step was to determine the exact cGMP concentration range in which only one functional subunit is activated by using global fits analyses with Markovian models.

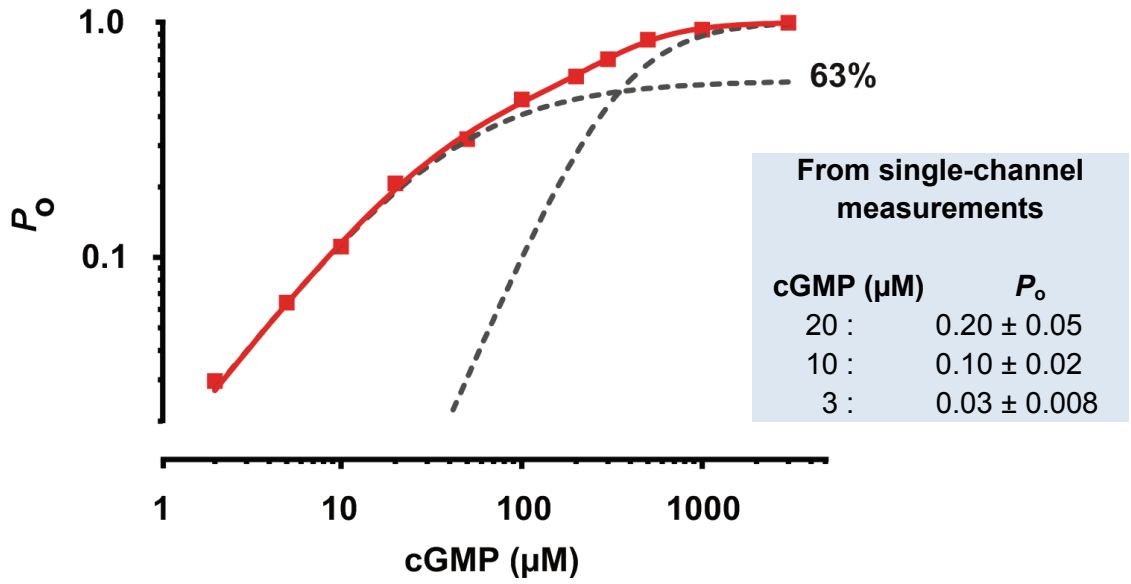

Figure 16. Open probabilities of *mut-mut-mut-wt* channel at different cGMP concentrations. The experimental data was well described by two Hill functions (red curve) as indicated by the dashed lines suggesting the presence of two components of high and low cGMP apparent affinity. The open probability values obtained from single-channel measurements in the presence of representative concentrations (3 µM, 10 µM and 20 µM) shown in the right panel were very similar with the ones obtained from macroscopic data.

5.6. Identification of the contribution of each individual subunit to channel activation by global fit analysis with Markovian models

It is well known that the CNG channel activation requires a cooperative interaction of its subunits which is triggered by the binding of cyclic nucleotides to the CNBDs (Biskup et al. 2007, Kaupp and Seifert 2002, Nache et al. 2005, Zufall et al. 1991). In addition, the steady-state concentration-response relationship of CNGA2 channels, yields a Hill coefficient of about two (Dhallan et al. 1990) or more than two (Kusch et al. 2010a, Bonigk et al. 1999), suggesting that the homotetrameric CNGA2 channel requires at least two ligands for fully opening. Moreover, evidence

from the single-channel analysis of rat olfactory CNGA2 channels confirmed the cooperative binding of at least two ligands at the binding sites in order to open the channels (Li and Lester 1999). However, so far, it is still unknown how each individual subunit works to translate ligand binding to the channel opening in the absence of cooperative effect from neighboring subunits even in the simple structure of the homotetrameric CNGA2 channels. To study the work of only one subunit is not easy due to interaction between the subunits. We showed in chapter 4.3. that $EC_{50,l}$ = 354.12 µM for *mut-mut-mut-wt*, describing the work of *mut* subunits, is only approximately half the value of $EC_{50,l}$ = 687.7 µM for *mut-mut-mut-mut* suggesting the existence of complex interactions between the *wt* and *mut* subunits.

To determine the contribution of each functional subunit (*wt*) upon ligand binding to channel gating, we performed a global fit analysis with five Markovian models (Figure 17A). The global fit analysis strategy used herein is considerably superior over the double mutant cycle analysis (Hidalgo and MacKinnon 1995) due to the fact that it includes all four mutations instead of only two and it considers the full shape of the concentration-response relationships. Assuming that occupying a low-affinity binding site is functionally equivalent to occupying a high-affinity binding site, the steady-state concentration-response relationships of the five concatemers *wt-wt-wt-wt*, *mut-wt-wt-wt*, *mut-mut-wt-wt*, *mut-mut-mut-wt* and *mut-mut-mut-mut* (Figure 17B) were simultaneously globally fitted by five respective Markovian models from 4*wt*-model to 0*wt*-model as shown in Figure 17A. These models are coupled by their equilibrium constants and the values for the closed-open isomerization. E_0 and E_4 were set to 1.7×10^{-5} and 9.9×10^{1} according to single-channel experiments. $K_{A1H} \ldots K_{A4H}$, $K_{A1L} \ldots K_{A4L}$ are the equilibrium association constants for the four high and low affinity binding sites (Table 4). We assumed $K_{A3H} = K_{A4H}$, $K_{A3L} = K_{A4L}$, and $E_3 = E_4$ to increase the fit constraints. The values are given as mean±SEM. CV% indicate the error in %. χ^2 was 123.91. These Markovian models could describe very closely the steady-state concentration response relationships. Using this approach we could characterize the apparent affinity of each binding domain (Table 4). Notably, the apparent affinity of the only

one *wt* subunit in the *mut-mut-mut-wt* channel was determined to be approximately 25 µM which correlates very well with the value obtained from macroscopic (44.34 µM, see Figure 11). The respective open-close isomerization is assumed to be caused by the entire pore with contributions of all four subunits.

When plotting for the 1*wt*-model the occupancy of the states as function of the cGMP concentration (Figure 18), we could show that at 3 µM the channel opening is generated by 94.6% by a single subunit (the high-affinity *wt*-subunit). Therefore, the contribution to channel activation of about ~17% could be attributed to the only *wt*-subunit in the *mut-mut-mut-wt* construct (O_1, the peak of red continuous line curve). By means of global fit analysis we were able to characterize with high accuracy the contribution of one subunit to channel activation without any interfering effects coming from the additional binding steps.

A

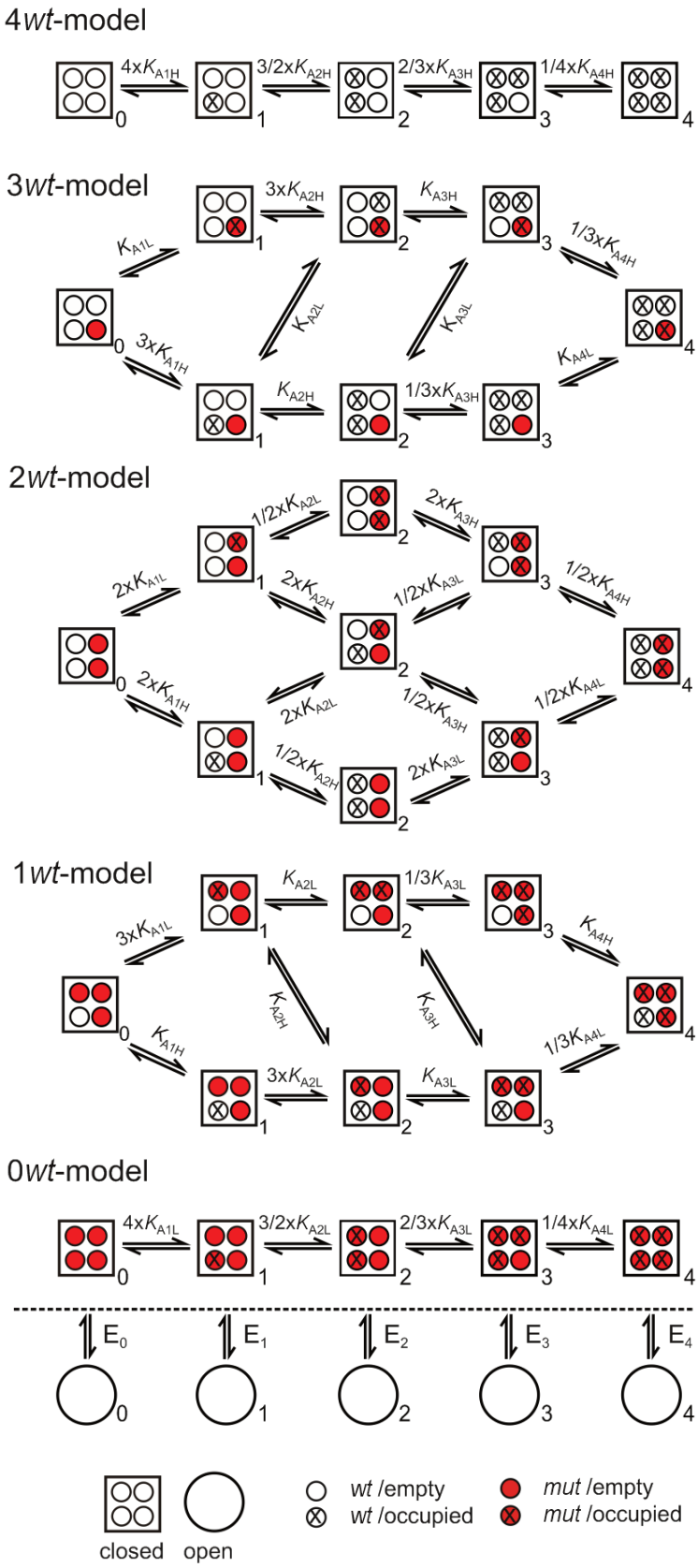
4wt-model
3wt-model
2wt-model
1wt-model
0wt-model
closed
open
wt /empty
wt /occupied
mut /empty
mut /occupied

B

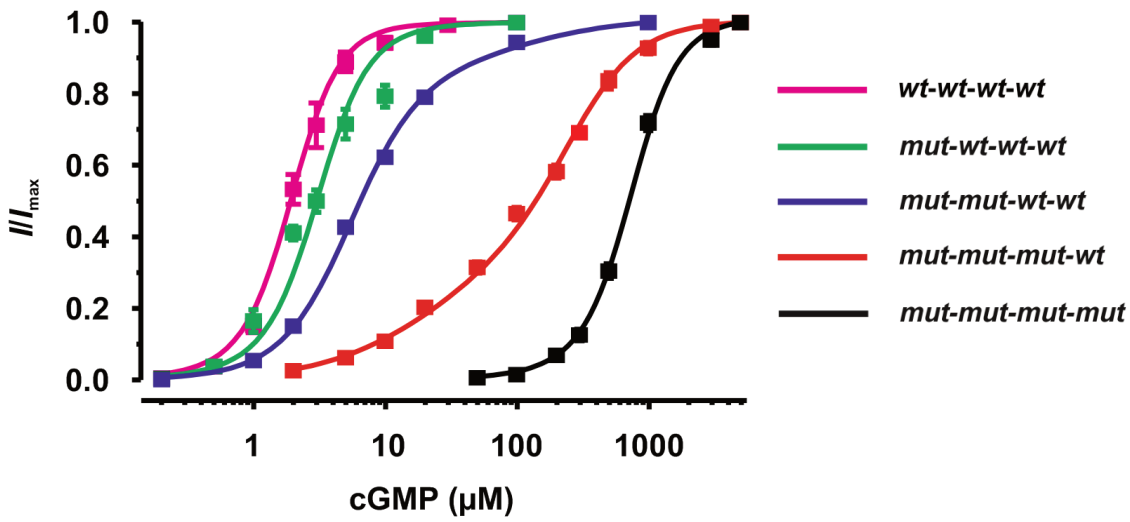

Figure 17. Global fit of concentration-response relationships from five concatemers. A) Five Markovian models (4*wt*-model, 3*wt*-model, 2*wt*-model, 1*wt*-model, 0*wt*-model) describing the activation gating of the *wt-wt-wt-wt*, *mut-wt-wt-wt*, *mut-mut-wt-wt*, *mut-mut-mut-wt*, and *mut-mut-mut-mut* concatemers, respectively. The squares represent closed states. The open states (big circles) and the three equilibrium constants for the closed-open isomerizations E_0, E_1, E_2, E_3, E_4 are indicated only once at the bottom. The white circles are high-affinity binding sites (*wt*) whereas the red circles are low-affinity binding sites (*mut*). An empty binding site is symbolized by an empty circle whereas an occupied binding site is symbolized by a cross. K_{A1H}, K_{A2H}, K_{A3H}, K_{A4H}, K_{A1L}, K_{A2L}, K_{A3L}, and K_{A4L} are the eight equilibrium association constants for the four high- and four low affinity binding sites, respectively. B) The five steady-state concentration-response relationships were globally fitted by the respective Markovian models. The fit was done by Sabine Hummert.

Table 4. Equilibrium constants determined by the global fit of five concentration-response relationships

Equilibrium constant	Dimension	Mean	SEM	CV%
K_{A1H}	M^{-1}	4.05×10^{4}	0.15×10^{4}	3.76
K_{A2H}	M^{-1}	7.90×10^{4}	0.65×10^{4}	8.26
$K_{A3H} = K_{A4H}$	M^{-1}	5.92×10^{4}	0.49×10^{4}	8.33
K_{A1L}	M^{-1}	1.03×10^{2}	0.04×10^{2}	4.18
K_{A2H}	M^{-1}	2.01×10^{2}	0.16×10^{2}	8.08
$K_{A3L} = K_{A4L}$	M^{-1}	1.51×10^{2}	0.12×10^{2}	8.06
E_0	-	1.70×10^{-5}	-	-
E_1	-	3.59×10^{-1}	0.14×10^{-1}	3.97
E_2	-	9.58×10^{0}	0.61×10^{0}	6.35
$E_3 = E_4$	-	9.90×10^{1}	-	-

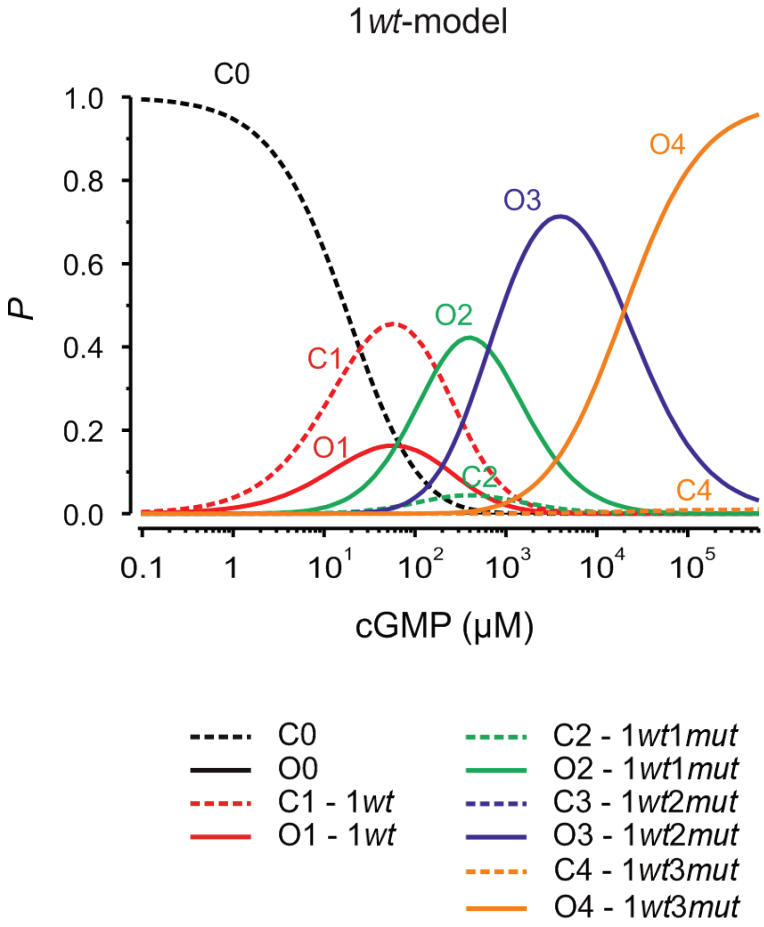

Figure 18. Occupancy of the states (*P*) as function of the cGMP concentration based on the 1*wt*-model for the *mut-mut-mut-wt* channel. The red continuous curve which represents the open probability caused by the first binding step (O1-1*wt*) indicates the concentration range (approximately 3 µM and below) where predominantly only one binding site is occupied. The dashed lines represent the respective close state.

5.7. The binding of the second ligand in *mut-mut-wt-wt* channels was able to switch the channel from a mostly closed to a fully open channel

The relationship between ligand binding to activation gating in homotetrameric CNGA2 channels was previously studied by means of patch-clamp fluorometry

using the fluorescent cGMP analogue 8-DY547-cGMP as the ligand (Biskup et al. 2007). It was shown that after the second ligand binding step, the channels showed nearly full opening (P_o was close to 1). These results suggest that the binding of the second ligand is the key step for the channel activation and the binding of the third and the forth ligand only drives the channel to a more stable open state.

Herein, we aimed not only to verify the previous results (Biskup et al. 2007) but also to directly show the effects of the second binding step at single-channel level in the *mut-mut-wt-wt* concatemeric construct. The *mut-mut-wt-wt* channel was expressed in oocytes and the measurements were performed in inside-out patches. The channels were activated by different cGMP concentrations: 1 µM, 3 µM, 10 µM, 25 µM and 1000 µM. We assumed that in the lower concentration range channel activation is triggered mainly by ligand binding to the two *wt* subunits only. Three representative single-channel traces for each cGMP concentration are shown in Figure 19.

In the absence of cGMP, P_o is very low $8.8 \times 10^{-4} \pm 4.8 \times 10^{-4}$ representing the spontaneous channel opening. At saturating cGMP concentration (1000 µM), P_o approaches unity with the value of 0.99 ± 0.003. The open probability increased following an increase of the cGMP concentration as follows: for 1 µM: $P_o = 0.18 \pm 0.07$; for 3 µM: $P_o = 0.26 \pm 0.11$; for 10 µM: $P_o = 0.76 \pm 0.11$; and for 25 µM: $P_o = 0.94 \pm 0.02$. Figure 20 shows the representative amplitude histograms which were fitted by the sum of two Gaussians functions with means as follows: 1 µM: $i = 4.58 \pm 0.14$ pA; 3 µM: $i = 4.59 \pm 0.34$ pA; 10 µM: $i = 4.73 \pm 0.08$ pA; 25 µM: $i = 4.72 \pm 0.11$ pA; 100 µM: $i = 4.84 \pm 0.16$ pA.

The results suggest that the amplitudes of the single-channel *mut-mut-wt-wt* current channels did not depend on the cGMP concentrations. We can also confirm the absence of subconductance levels even after two binding steps. The herein determined single-channel parameters are summarized in Table 5.

To be able to precisely determine up to which concentration only the two *wt*-subunits of the *mut-mut-wt-wt* channel are activated, we determined the occupancy probability of the states as function of the cGMP concentration using the 2*wt*-model (Figure 17A). We found that in the cGMP concentration range up to 10 µM, binding

occurs predominantly only to two *wt* subunits (Figure 21). The contribution to channel activation of about ~74% could be attributed to only two *wt* subunits in the *mut-mut-wt-wt* construct (Figure 21, see the peak of green continuous curve).

Our results indicate that the second ligand binding step is a very important step for channel activation, triggering the channel to a switch from mostly closed to a fully open state. The third and the fourth binding steps have a smaller contribution to channel opening (0.6% and 24.3% respectively), confirming that the third and the fourth binding step only stabilize the open state.

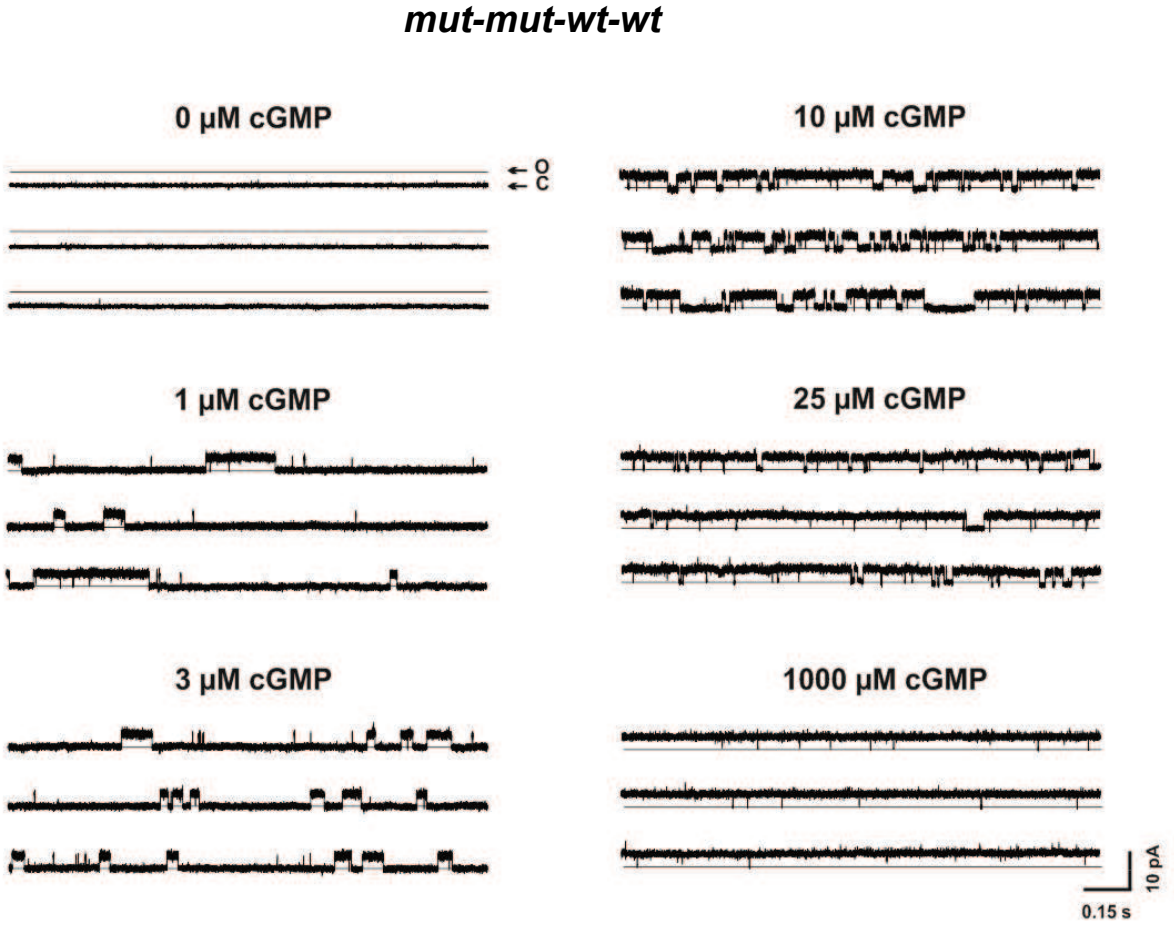

Figure 19. Representative single-channel traces of *mut-mut-wt-wt* construct at different cGMP concentrations. The membrane voltage was clamped at +100 mV. All subunits (*wt* and *mut*) were activated at the saturating concentration of 1000 µM cGMP. The open channel (o) and closed channel level (c) are indicated by arrows.

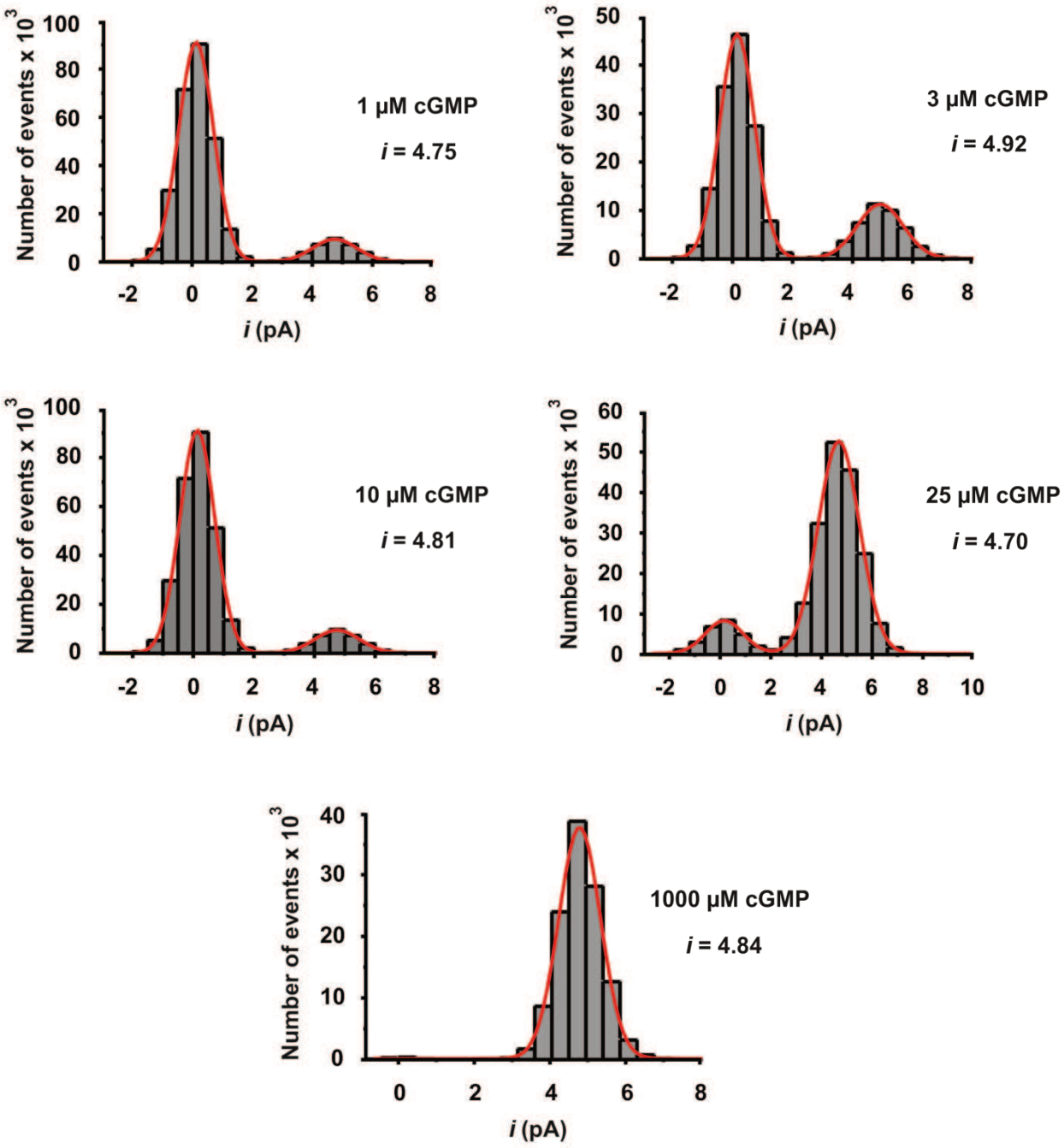

Figure 20. All points amplitude histograms of *mut-mut-wt-wt* at different cGMP concentrations. The representative amplitudes of the single-channel current at 1 μM, 3 μM, 10 μM, 25 μM and 1000 μM, are not significantly different (one-way ANOVA test, $p = 0.84$).

Table 5. Open probability and single-channel current amplitude for *mut-mut-wt-wt* channel at different cGMP concentrations

cGMP (μM)	*i* (pA)	P_o	*N*
0	-	$8.8x10^{-4} \pm 4.8x10^{-4}$	8
1	4.58 ± 0.14	0.18 ± 0.07	5
3	4.59 ± 0.34	0.26 ± 0.11	5
10	4.73 ± 0.08	0.76 ± 0.11	4
25	4.72 ± 0.11	0.94 ± 0.02	4
1000	4.84 ± 0.16	0.99 ± 0.003	6

Parameters are shown as mean ± SEM values. P_o is the open probability. *N* is the number of experiments.

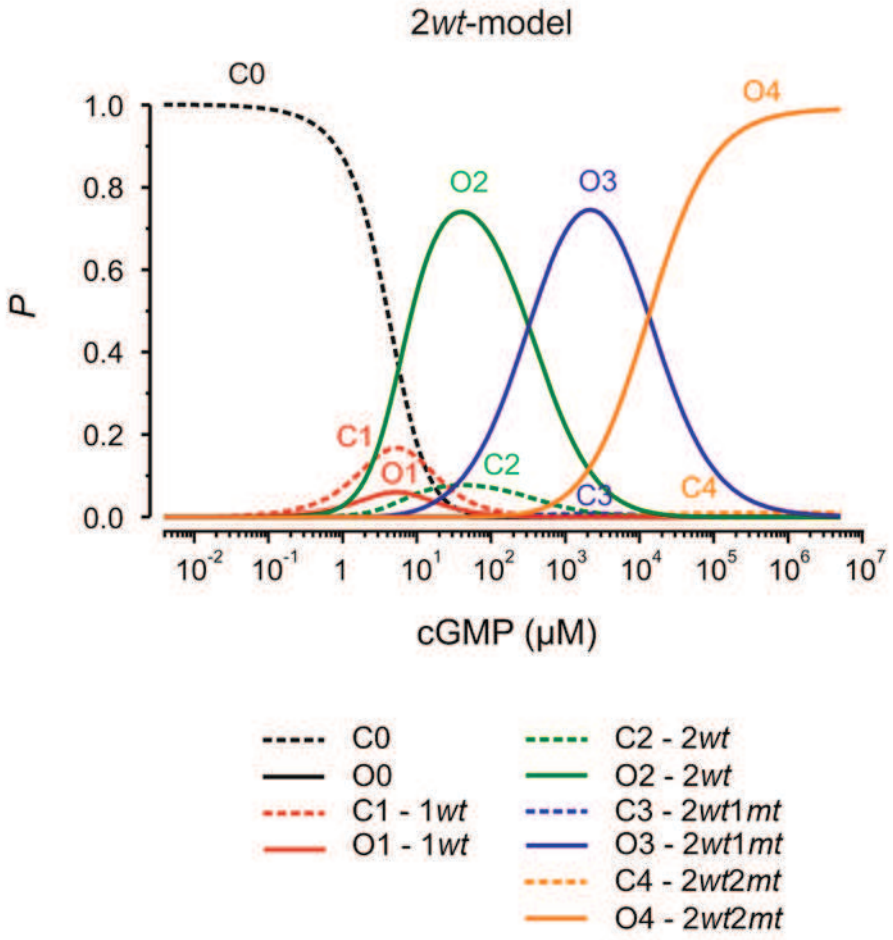

Figure 21. Occupancy of the states (*P*) as function of the cGMP concentration based on the 2*wt*-model for the *mut-mut-wt-wt* channel. The green continuous curve which represents the open probability caused by the second binding step (O2-2*wt*) indicates the concentration range (approximately 10 µM and below) where only the two *wt*-subunits were predominantly occupied. The dashed lines represent the respective close states.

6. Discussion

Despite the fact that the subunit composition in olfactory CNGA2 channels is very simple the molecular process of the translation of ligand binding to channel gating in these channels is still unclear. Nevertheless, what is well agreed upon is that the channel function is not based on independently operating but strongly interacting subunits. This interaction process is generally called cooperativity. It was previously shown that the activation of CNGA2 channels is highly cooperative (Biskup et al. 2007, Nache et al. 2005). However, it is still a mystery how the first ligand binds to an empty channel and how the channel activation proceeds. In this study, we provided the first insight into the action of a single subunit without superimposing cooperative effects by the other subunits in a homotetrameric CNGA2 channel.

6.1. The concatenation technique does not hinder the channel function

Previous works on CNG concatenated subunits have focused on lower order concatemers, mostly dimers, which were further coexpressed with additional subunits, thereby leading to equivocal interpretations (He et al. 2000, Liu et al. 1998, Shapiro and Zagotta 1998). Studies of tandemly linked dimers consisting of *mut* and *wt* subunits have provided direct evidence for the cooperative gating mechanism of CNG channels (Goulding et al. 1994, Varnum and Zagotta 1996) and K^+ channels (Tytgat and Hess 1992, Schoppa et al. 1992, McCormack et al. 1994). However, this approach cannot address properly the question how an individual subunit contributes to channel activation. One disadvantage of the dimeric linkage of subunits has been observed by McCormack and co-workers in their work on Shaker K^+ channels (McCormack et al. 1992). They reported that the Shaker K^+ channels formed by expressing dimers of *wt*-subunits and a truncated non-functional subunit (Sh^{102}) yielded much higher currents than they expected.

They suggest that the channels built by the *wt*-Sh^{102} dimeric construct do not form the tetrameric channels with the expected subunit stoichiometry due to these reasons: (1) The phenotype of the *wt*-subunit seems to be predominant. Therefore, it is more likely to assemble into a functional channel than the Sh^{102} subunit; (2) The expression of Shaker K^+ channels formed by coinjection of *wt* with Sh^{102} cRNA was suppressed but did not decrease the expression of coinjection of Na^+ channel with Sh^{102} cRNA (McCormack et al. 1991), probably because of the nature of a specific interaction between *wt* with Sh^{102} subunits. In summary, this tandem dimeric strategy could not always guarantee a uniform subunit stoichiometry.

One possibility to overcome the limitation of tandem dimeric strategy was to concatenate all four subunits. The first CNGA2 channel formed from four concatenated subunits was successfully constructed by Chan and Young, 2009. They presented evidence for a bimodal agonism in heteromeric CNG channels. This means that at concentrations above 3 mM the channel open probability increases with initial cGMP binding events but decreases with subsequent binding events (Chan and Young 2009).

We applied the concatenation technique to homotetrameric CNGA2 channels. Our aim was to dissect the work of a single subunit in a functional homotetrameric channel. The CNGA2 subunits were linked together by means of a short linker (Glysine-Serine-Alanine). We first performed the necessary control experiments to investigate whether the concatemers were structurally intact and the functional properties of the channel were not influenced by this approach.

We present three pieces of evidence supporting that the CNGA2 concatemeric constructs formed functional channels and a breakdown of the concatemers to individual subunits did not occur. First, from macroscopic measurements we showed that the concentration-response relationships of the concatameric channels containing either *wt* subunits or *mut* subunits (*wt-wt-wt-wt* and *mut-mut-mut-mut*) fully match those of the respective channels built from their monomers (Figure 6 and Figure 11). These data indicate that the concatemeric constructs produce functional channels and that the concatemers composed of *wt* or *mut* subunits retain the fundamental functional characteristics of the respective

channels formed from *wt* or *mut* monomers. Moreover, the concatenation technique does not significantly distort the channel function. Additionally, when substantially decreasing the number of functional binding sites by means of a point mutation (R538E) we observed also a graded decrease in the channel cGMP sensitivity (for *wt-wt-wt-wt*: EC_{50} =1.97; for *mut-wt-wt-wt*: EC_{50} = 2.87; for *mut-mut-wt-wt*: EC_{50} = 6.79; for *mut-mut-mut-wt*: $EC_{50,l}$ = 354.12 and for *mut-mut-mut-mut*: EC_{50} = 687.7). Taken together, these results provide strong evidence that all concatemeric channels were formed by continuous peptides with the expected subunits. In addition, all four subunits were reliably incorporated in the full assembly as tetrameric concatemers.

Second, the single-channel activity of the *wt-wt-wt-wt* channels was assayed and compared with that of the *wt* channels to investigate whether linking of the subunits affects the single-channel current amplitude and the channel open probability. At respectively saturating cGMP concentrations, the single-channel current amplitude of the *wt-wt-wt-wt* channels was similar to that of the 4*wt* channels (for 4*wt*: i = 4.99 ± 0.43 pA and for *wt-wt-wt-wt*: i = 5.11 ± 0.24 pA). Also, the open probability of the concatemeric channels was identical to that of the channels formed by monomers (for 4*wt*: P_o = 0.99 ± 0.002 and for *wt-wt-wt-wt*: P_o = 0.99 ± 0.002) as shown in Figure 7. These results also confirm that the concatenation technique does not have any impact on the channel function even at the single-channel level. The concatenated channels with the expected subunit stoichiometry were successfully incorporated into the plasma membrane.

Third, the concentration-response relationship of the *wt-wt-wt-wt* channel coexpressed with an excess of a mutant monomer (*mut*) (EC_{50} = 61.24 µM, H = 2.15) was indistinguishable from that of the *wt-wt-wt-wt channel alone* (EC_{50} = 56.17 µM, H = 1.90; Figure 10). These data suggest that the *mut* monomer subunits did not form functional channels with the linked subunits and the concatemeric CNGA2 channel contained the correct complement of functional subunits. Also, they confirm that the CNG channels are not pentameric but tetrameric channels as previously reported based on single-channel conductance of dimers (Liu et al. 1998).

Moreover, these results indicate that the presence of the linkers, which were used for linking the subunits and their length, did not influence the ligand sensitivity, the cooperativity between subunits as well as the single-channel properties. It was previously shown that the length of the linker might influence the channel function (Zhou et al. 2003, Baumann et al. 2001). For example, in the nicotinic acetylcholine receptor a dimer can link two pentamers due to too long linkage, thereby causing the formation of unexpected functional receptors (Zhou et al. 2003). Therefore, it is indicated to keep the linker length as short as possible in order to minimize eventual side effects (Minier and Sigel 2004). Proteolysis within the linkers of the concatemeric constructs could also occur, generating undesired by-products. For example, studies in P2X receptors showed evidence for this proteolysis which results in the presence of monomeric and dimeric byproducts (Nicke et al. 2003).
In conclusion, we provide compelling evidence that not only the concatemers were intact but also that this experimental approach is appropriate to study specific gating effects of individual channel subunits.

6.2. The number but not the position of the functional subunit(s) in the tetrameric concatemers detemine channel activation

Homotetrameric CNGA2 channels are tetramers and up to date, by using conventional expression techniques, it is impossible to study one functional subunit at a time and to choose the position of the respective subunit. We overcome this problem by using concatemeric constructs which allow us to constrain the number and position of the functional subunits as we desire. We asked the question how does the number of the functional subunit(s) in tetrameric concatemers influence the channel function? We showed that the concatemers containing 1, 2, 3, or 4 disabled subunits showed a progressive loss of the cGMP sensitivity (EC_{50}), indicating that a graded loss of functional binding domains leads to a gradual decease of the channel apparent affinity. A systematic decrease of the Hill-coefficient was also observed (Figure 12B), suggesting decreased cooperativity between subunits depending on the number of functional binding sites.

Conclusively, the number of the functional subunit(s) in tetrameric CNGA2 channels has a great impact on the channel function.

Similar observations were also found in several previous reports. The study of the effects of mutations in individual subunits on voltage-dependent potassium channel (RBK1, rat Kv1.1) activation produced similar results. By means of the concatenation technique, the authors showed that changes in the number but not the position(s) of mutated subunits altered the free energy of dissociation of tetraethylammonium from RBK1 tetrameric channels (Hurst et al. 1992). The subunit stoichiometry of the Kir1.1 channel in proton-dependent gating was also studied by using the concatenation technique. An increase in the number of K80M mutant subunits caused graded loss of pH-dependency in channel gating (Wang et al. 2005).

To characterize the interaction between neighbored channel subunits we tested the effect of the position of the functional subunit(s) in concatemeric CNGA2 channels containing a different number of mutated binding sites on the channel function. We first addressed the question: Do channels formed from tandem dimers with only two functional subunits (*wt-mut* and *mut-wt*) respond similarly to cGMP? The concentration-response relationships of those two constructs showed similar cGMP sensitivity and Hill coefficient (for *wt-mut*: EC_{50} = 6.78, H = 1.51; for *mut-wt*: EC_{50} = 6.11, H = 1.23). These results provide two important implications regarding assembly and subunit stoichiometry. First, both *wt* and *mut* subunits in a dimer were indeed incorporated into a full assembled channel without hanging subunits. Otherwise the two tandem dimers should show different cGMP sensitivity. Second, it indicates that the position of the subunits in dimers is not important for channel function. Changing the position of the functional subunit(s) within the tetrameric concatemers did not change the channel activity (Figure 13). Concatemers containing two *wt*-subunits which were situated either diagonally (*trans* configuration: for *wt-mut-wt-mut*: EC_{50} = 8.76, H = 1.20 and for *mut-wt-mut-wt*: EC_{50} = 8.61, H = 1.34) or adjacent to each other (*cis* configuration: for *mut-mut-wt-wt:* EC_{50} = 6.79, H = 1.30; for *wt-wt-mut-mut*: EC_{50} = 7.74, H = 1.31) showed a similar cGMP sensitivity (Figure 13A). This indicates that it is not the interaction between

the neighboring subunits but only the number of binding steps that has the major impact on the channel function.

These data are inconsistent with a dimer of dimer model previously used to describe the activation of CNG channels which suggests that the CNG channel is composed of two functional dimers (Liu et al. 1998). For HCN channels, Ulens and Siegelbaum reported that a dimer of dimer model adequately described how subunits interact during HCN2 channel gating because *trans* channels showed a greater response to cAMP than *cis* channels (Ulens and Siegelbaum 2003).

6.3. CNGA2 channels are able to open after the first ligand binding step

Previously, the concentration-response relationships of CNGA2 channels consistently generated Hill coefficients (a measure of apparent cooperativity) of two (Dhallan et al. 1990) or larger (Kusch et al. 2010a, Bonigk et al. 1999), suggesting that the binding of at least two ligands is required to obtain full channel activation. The gating mechanism of CNGA2 channels is a cooperative action of subunits described by allosteric coupling between ligand binding and channel gating (Dhallan et al. 1990, Kaupp and Seifert 2002). Subsequently, the analysis of single-channel activity of homotetrameric CNGA2 channels indicated also that at least two ligands are required for channel activation (Li and Lester 1999). Later, using flash photolysis-induced jumps of cyclic-nucleotide concentration a novel gating mechanism for CNG channels with three highly cooperative binding steps was proposed (Nache et al. 2005). Following this line, by means of patch-clamp fluorometry and laser scanning microscopy (Kusch et al. 2010b, Biskup et al. 2007), Biskup et al. extended this kinetic model and developed a more accurate kinetic scheme for homotetrateric CNGA2 channels. This model includes 4 binding steps and shows a significant interaction between the binding sites. Already the second binding step is the switch that fully opens the channel, whereas the third and the fourth binding step only stabilizes the open channel (Biskup et al. 2007).

All previous studies of the translation of ligand binding to channel gating in multimeric allosteric proteins suggested a complex cooperativity between subunits. However, the precise work of only one functional subunit without any cooperative effects from neighboring subunits has not been studied until now.

We showed evidence and characterize the contribution of an individual binding event to channel activation at both single-channel and macroscopic levels in concatemeric CNGA2 channels. The most important finding of this study is that only one functional subunit is necessary to evoke channel activation when in the presence of cGMP. To analyze the work of a single functional subunit in an otherwise non-liganded channel we chose the *mut-mut-mut-wt* construct as being representative for all concatemeric constructs with one *wt* subunit because the *wt* subunit has a free C-terminus with its cyclic nucleotide-binding domain (CNBD). At the macroscopic level, our results show that a single CNGA2 subunit operated a channel only at 23-fold higher cGMP concentration that a tetrameric CNGA2 channel consisting of four cooperative subunits (Figure 11). In addition, we observed that after the first binding step the channels reached approximately 63% of its full opening as shown in Figure 16. Nevertheless, one should keep in mind that from a certain cGMP level the contribution of the first binding step could be influenced by the second binding step as well. Therefore, we performed a global fit analysis with Markovian models to exactly determine the contribution of the first ligand binding step.

6.4. A global fit analysis with five Markovian models described well the respective steady-state concentration-response relationships

Makovian models have been successfully applied in several previous studies in order to characterize elementary gating machanisms of CNGA2 (Nache et al. 2013, Biskup et al. 2007) and HCN2 pacemaker channels (Kusch et al. 2012). However, the present global fit strategy (Figure 17) significantly differs from the previous fit approaches because it analyzes five concentration-response relationships of concatemers with zero to four *wt*-subunits and uses five corresponding kinetic schemes that were strictly coupled by the equilibrium association constants. The advantage of this strategy is that it involves the corresponding number of four to zero *mut*-subunits which do not only pull the concentration-response relationships apart but also characteristically shape them. This plenty of information from the global fit strategy allowed us to characterize the action of each subunit (*wt* or *mut*), their apparent affinity and their contribution to channel activation. The respective Markovian models could describe well the five steady-state concentration-response relationships (Figure 17). In addition, the 1 *wt*-model allowed us to characterize the work of a single subunit embedded in a working channel, in particular how a subunit works without any cooperative effects arising from its neighbors. Based on the 1*wt*-model for the *mut-mut-mut-wt* channel the determined apparent affinity of the first binding step is approximately 25 µM cGMP. This suggests that the high apparent affinity of the homotetrameric channel (~1.9 µM cGMP) is the result of the cooperativity between subunits.

We could show that up to 3 µM cGMP the ligand binding proceeds mainly to the only one *wt* subunit (Figure 18). Therefore we could characterize the single-channel activity triggered by the first binding step only in the *mut-mut-mut-wt* channel. The single-channel measurements allowed us to observe the work of a single subunit embedded in a channel. Binding to the single *wt*-subunit triggered the opening of the channel pore to the full conductance level. No subconductance levels were observed (Figure 14). This finding suggests that the channel pore with

its structural contributions of all four subunits works solely as a whole and that an increasing number of occupied binding sites only enhance the open probability. This conclusion is consistent with kinetic models of the Monod-Wyman-Changeux type (Monod et al. 1965), containing only one concerted opening step of all subunits (Biskup et al. 2004, Goulding et al. 1994). And, this conclusion is inconsistent with kinetic models of Koshland-Nemethy-Filmer type (Koshland et al. 1966), assuming independent opening steps of the subunits (Karpen and Ruiz 2002). In this study, the open-closed isomerization in all respective Markovian models (Figure 17A) is assumed to be caused by the whole pore with contributions of all four subunits. Additional higher cGMP concentrations increase the open probability due to the rising recruitment of these open-close isomerizations (Nache et al. 2013).

However, the opening behavior of *mut-mut-mut-wt* channels is different from that obtained from rod CNGA1 channels activated with a fixed number of bound ligands (Ruiz und Karpen 1999). They reported that when one ligand binds to the rod CNG channel, the channel opened with a low conductance level and with very low open probability which was not significantly different from the spontaneous channel opening observed in the absence of cyclic nucleotides.

Interestingly, although the potassium-selective cyclic nucleotide-gated (CNGK) channel identified in sea urchin sperm (Bonigk et al. 2009, Strunker et al. 2006, Galindo et al. 2007) has several characteristics similar to the retinal and olfactory CNG channels, the ligand binding and channel gating in this prokaryotic CNG channel proceeds in a non-cooperative manner (Clayton et al. 2004, Altieri et al. 2008, Bonigk et al. 2009). Functional and structural studies have shown that their four CNBDs are not functionally equivalent and some of them might be not functional. Disabling each of the four CNBDs by mutagenesis indicated that the binding of a single cGMP molecule to the CNBD at repeat 3 is necessary and sufficient to open the channels in the absence of any major cooperative effects. The cGMP molecules probably either do not bind to the other CNBDs or the ligand binding is not translated to channel gating (Bonigk et al. 2009).

6.5. The second binding step induces almost full channel opening

By simultaneously measuring ligand binding and channel activation, previous work in our group showed that the second ligand binding switches the channels to an almost fully open state (Biskup et al. 2007). This work suggests that the second ligand binding is the key event for channel activation. Therefore, we wanted to confirm this previous finding and we characterized the contribution of the second ligand binding to channel activation using the concatemer containing only two functional subunits (*mut*-*mut*-*wt*-*wt*).

The combination of concatenation technique and global fit with Makovian models allowed us to investigate very accurately the effect of the second binding step on the channel activation. We showed that up to 10 µM cGMP the ligand binding process mainly occurred to the two *wt*-subunits in the *mut*-*mut*-*wt*-*wt* channel (Figure 21). We also showed that the second ligand binding step induces almost full channel activation which is supported by two results. First, from single-channel recording the two occupied functional subunits could open the channel by approximately 76% (Table 5, at 10 µM). Second, by means of the 2*wt*-model the cGMP binding to two *wt*-subunits contributes to channel activation by approximately 74% (Figure 21, see the peak of continuous green). The third and the fourth binding steps have only a minor contribution to the channel openness (Figure 21).

What is the physiological meaning of the first binding step in a tetrameric CNGA2 ion channel to evoke channel activation? Although we studied the contribution of the first binding step in concatemeric CNGA2 channels, our results are most likely also valid for non-concatenated channels, as well as for the native CNG channels composed of two CNGA2 subunits together with one CNGA4 and one CNGB1b subunit (Dhallan et al. 1990, Kaupp and Seifert 2002). The natural ligand of olfactory CNG channels is cAMP. It is well known that the cAMP concentration is typically in the low micromolar range (Breer et al. 1990). Therefore, at low micromolar cAMP concentration and in a small compartment such as cilia, a single cAMP molecule binding to an empty channel can be expected to appear regularly.

In conclusion, the findings described herein might be of relevance also under physiological conditions. Nevertheless, one should be aware that in the low micromolar cAMP range, relevant channel activity still requires the cooperative process of the liganded subunit with the other functional non-liganded subunits. It would therefore be attractive to perform similar experiments as reported herein with heterotetrameric concetemers.

7. Conclusion

1. By means of both macroscopic and single-channel measurements, we showed that concatenation of the subunits does not eventually influence CNGA2 channel function.

2. The number but not the position of the functional subunit(s) in the tetrameric CNGA2 concatemers influence channel activation.

3. Only one activated subunit can trigger noticeable channel activity and there is only one stable conductance level in the single-channel recordings.

4. The binding of the second ligand causes almost full CNGA2 channel opening. Moreover, the binding of the third and the fourth ligand has minor contributions only to open the channel pore. Probably, they only stabilize the channel open conformation (Biskup et al. 2007).

8. References

Akhtar S, Shamotienko O, Papakosta M, Ali F, Dolly JO. 2002. Characteristics of brain Kv1 channels tailored to mimic native counterparts by tandem linkage of alpha subunits: implications for K^+ channelopathies. J Biol Chem, 277 (19):16376-16382.

Altieri SL, Clayton GM, Silverman WR, Olivares AO, De la Cruz EM, Thomas LR, Morais-Cabral JH. 2008. Structural and energetic analysis of activation by a cyclic nucleotide binding domain. J Mol Biol, 381 (3):655-669.

Bakalyar HA, Reed RR. 1990. Identification of a specialized adenylyl cyclase that may mediate odorant detection. Science, 250 (4986):1403-1406.

Baker H, Cummings DM, Munger SD, Margolis JW, Franzen L, Reed RR, Margolis FL. 1999. Targeted deletion of a cyclic nucleotide-gated channel subunit (OCNC1): biochemical and morphological consequences in adult mice. J Neurosci, 19 (21):9313-9321.

Baumann SW, Baur R, Sigel E. 2001. Subunit arrangement of gamma-aminobutyric acid type A receptors. J Biol Chem, 276 (39):36275-36280.

Baur R, Minier F, Sigel E. 2006. A GABA(A) receptor of defined subunit composition and positioning: concatenation of five subunits. FEBS Lett, 580 (6):1616-1620.

Biel M, Michalakis S. 2007. Function and dysfunction of CNG channels: insights from channelopathies and mouse models. Mol Neurobiol, 35 (3):266-277.

Biskup C, Kusch J, Schulz E, Nache V, Schwede F, Lehmann F, Hagen V, Benndorf K. 2007. Relating ligand binding to activation gating in CNGA2 channels. Nature, 446 (7134):440-443.

Biskup C, Bohmer A, Pusch R, Kelbauskas L, Gorshokov A, Majoul I, Lindenau J, Benndorf K, Bohmer FD. 2004. Visualization of SHP-1-target interaction. J Cell Sci, 117 (Pt 21):5165-5178.

Blount P, Sukharev SI, Moe PC, Schroeder MJ, Guy HR, Kung C. 1996. Membrane topology and multimeric structure of a mechanosensitive channel protein of Escherichia coli. EMBO J, 15 (18):4798-4805.

Bonigk W, Altenhofen W, Muller F, Dose A, Illing M, Molday RS, Kaupp UB. 1993. Rod and cone photoreceptor cells express distinct genes for cGMP-gated channels. Neuron, 10 (5):865-877.

Bonigk W, Bradley J, Muller F, Sesti F, Boekhoff I, Ronnett GV, Kaupp UB, Frings S. 1999. The native rat olfactory cyclic nucleotide-gated channel is composed of three distinct subunits. J Neurosci, 19 (13):5332-5347.

Bonigk W, Loogen A, Seifert R, Kashikar N, Klemm C, Krause E, Hagen V, Kremmer E, Strunker T, Kaupp UB. 2009. An atypical CNG channel activated by a single cGMP molecule controls sperm chemotaxis. Sci Signal, 2 (94):ra68.

Borisy FF, Ronnett GV, Cunningham AM, Juilfs D, Beavo J, Snyder SH. 1992. Calcium/calmodulin-activated phosphodiesterase expressed in olfactory receptor neurons. J Neurosci, 12 (3):915-923.

Bos JL. 2006. Epac proteins: multi-purpose cAMP targets. Trends Biochem Sci, 31 (12):680-686.

Bradley J, Frings S, Yau KW, Reed R. 2001. Nomenclature for ion channel subunits. Science, 294 (5549):2095-2096.

Bradley J, Li J, Davidson N, Lester HA, Zinn K. 1994. Heteromeric olfactory cyclic nucleotide-gated channels: a subunit that confers increased sensitivity to cAMP. Proc Natl Acad Sci U.S.A., 91 (19):8890-8894.

Brady JD, Rich ED, Martens JR, Karpen JW, Varnum MD, Brown RL. 2006. Interplay between PIP3 and calmodulin regulation of olfactory cyclic nucleotide-gated channels. Proc Natl Acad Sci U.S.A., 103 (42):15635-15640.

Breer H, Boekhoff I, Tareilus E. 1990. Rapid kinetics of second messenger formation in olfactory transduction. Nature, 345 (6270):65-68.

Brown KM, Dennis JE. 1972. Derivative-free analogues of the Levenberg-Marquardt and Gauss algorithmus or nonlinear least squares approximation. 1972, 18:289-297.

Brunet LJ, Gold GH, Ngai J. 1996. General anosmia caused by a targeted disruption of the mouse olfactory cyclic nucleotide-gated cation channel. Neuron, 17 (4):681-693.

Buck L, Axel R. 1991. A novel multigene family may encode odorant receptors: a molecular basis for odor recognition. Cell, 65 (1):175-187.

Chan KS, Young EC. 2009. Bimodal agonism in heteromeric cyclic nucleotide-gated channels. Channels (Austin), 3 (6):427-436.

Chen TY, Takeuchi H, Kurahashi T. 2006. Odorant inhibition of the olfactory cyclic nucleotide-gated channel with a native molecular assembly. J Gen Physiol, 128 (3):365-371.

Chen TY, Peng YW, Dhallan RS, Ahamed B, Reed RR, Yau KW. 1993. A new subunit of the cyclic nucleotide-gated cation channel in retinal rods. Nature, 362 (6422):764-767.

Clayton GM, Silverman WR, Heginbotham L, Morais-Cabral JH. 2004. Structural basis of ligand activation in a cyclic nucleotide regulated potassium channel. Cell, 119 (5):615-627.

Coburn CM, Bargmann CI. 1996. A putative cyclic nucleotide-gated channel is required for sensory development and function in C. elegans. Neuron, 17 (4):695-706.

Craven KB, Zagotta WN. 2006. CNG and HCN channels: two peas, one pod. Annu Rev Physiol, 68:375-401.

Delay R, Restrepo D. 2004. Odorant responses of dual polarity are mediated by cAMP in mouse olfactory sensory neurons. J Neurophysiol, 92 (3):1312-1319.

Dhallan RS, Yau KW, Schrader KA, Reed RR. 1990. Primary structure and functional expression of a cyclic nucleotide-activated channel from olfactory neurons. Nature, 347 (6289):184-187.

Dumont JN. 1972. Oogenesis in Xenopus laevis (Daudin). I. Stages of oocyte development in laboratory maintained animals. J Morphol, 136 (2):153-179.

Emerick MC, Fambrough DM. 1993. Intramolecular fusion of Na pump subunits assures exclusive assembly of the fused alpha and beta subunit domains into a functional enzyme in cells also expressing endogenous Na^+ pump subunits. J Biol Chem, 268 (31):23455-23459.

Fesenko EE, Kolesnikov SS, Lyubarsky AL. 1985. Induction by cyclic GMP of cationic conductance in plasma membrane of retinal rod outer segment. Nature, 313 (6000):310-313.

Firestein S. 2001. How the olfactory system makes sense of scents. Nature, 413 (6852):211-218.

Firsov D, Gautschi I, Merillat AM, Rossier BC, Schild L. 1998. The heterotetrameric architecture of the epithelial sodium channel (ENaC). EMBO J, 17 (2):344-352.

Frings S, Lynch JW, Lindemann B. 1992. Properties of cyclic nucleotide-gated channels mediating olfactory transduction. Activation, selectivity, and blockage. J Gen Physiol, 100 (1):45-67.

Frings S, Seifert R, Godde M, Kaupp UB. 1995. Profoundly different calcium permeation and blockage determine the specific function of distinct cyclic nucleotide-gated channels. Neuron, 15 (1):169-179.

Gagnon DG, Bezanilla F. 2009. A single charged voltage sensor is capable of gating the Shaker K^+ channel. J Gen Physiol, 133 (5):467-483.

Galindo BE, de la Vega-Beltran JL, Labarca P, Vacquier VD, Darszon A. 2007. Sp-tetraKCNG: A novel cyclic nucleotide gated K^+ channel. Biochem Biophys Res Commun, 354 (3):668-675.

Ganetzky B, Robertson GA, Wilson GF, Trudeau MC, Titus SA. 1999. The eag family of K^+ channels in Drosophila and mammals. Ann N Y Acad Sci, 868:356-369.

Gerstner A, Zong X, Hofmann F, Biel M. 2000. Molecular cloning and functional characterization of a new modulatory cyclic nucleotide-gated channel subunit from mouse retina. J Neurosci, 20 (4):1324-1332.

Giorgetti A, Nair AV, Codega P, Torre V, Carloni P. 2005. Structural basis of gating of CNG channels. FEBS Lett, 579 (9):1968-1972.

Gordon SE, Zagotta WN. 1995. A histidine residue associated with the gate of the cyclic nucleotide-activated channels in rod photoreceptors. Neuron, 14 (1):177-183.

Goulding EH, Tibbs GR, Siegelbaum SA. 1994. Molecular mechanism of cyclic-nucleotide-gated channel activation. Nature, 372 (6504):369-374.

Groot-Kormelink PJ, Broadbent S, Beato M, Sivilotti LG. 2006. Constraining the expression of nicotinic acetylcholine receptors by using pentameric constructs. Mol Pharmacol, 69 (2):558-563.

Hamill OP, Marty A, Neher E, Sakmann B, Sigworth FJ. 1981. Improved patch-clamp techniques for high-resolution current recording from cells and cell-free membrane patches. Pflugers Arch, 391 (2):85-100.

Haynes L, Yau KW. 1985. Cyclic GMP-sensitive conductance in outer segment membrane of catfish cones. Nature, 317 (6032):61-64.

He Y, Ruiz M, Karpen JW. 2000. Constraining the subunit order of rod cyclic nucleotide-gated channels reveals a diagonal arrangement of like subunits. Proc Natl Acad Sci U.S.A., 97 (2):895-900.

Hidalgo P, MacKinnon R. 1995. Revealing the architecture of a K^+ channel pore through mutant cycles with a peptide inhibitor. Science, 268 (5208):307-310.

Hurst RS, Kavanaugh MP, Yakel J, Adelman JP, North RA. 1992. Cooperative interactions among subunits of a voltage-dependent potassium channel. Evidence from expression of concatenated cDNAs. J Biol Chem, 267 (33):23742-23745.

Isacoff EY, Jan YN, Jan LY. 1990. Evidence for the formation of heteromultimeric potassium channels in Xenopus oocytes. Nature, 345 (6275):530-534.

Jan LY, Jan YN. 1990. A superfamily of ion channels. Nature, 345 (6277):672.

Janssens A, Voets T. 2011. Ligand stoichiometry of the cold- and menthol-activated channel TRPM8. J Physiol, 589 (Pt 20):4827-4835.

Jones DT, Reed RR. 1989. Golf: an olfactory neuron specific-G protein involved in odorant signal transduction. Science, 244 (4906):790-795.

Kaneko H, Putzier I, Frings S, Kaupp UB, Gensch T. 2004. Chloride accumulation in mammalian olfactory sensory neurons. J Neurosci, 24 (36):7931-7938.

Karpen JW, Ruiz M. 2002. Ion channels: does each subunit do something on its own? Trends Biochem Sci, 27 (8):402-409.

Karpen JW, Zimmerman AL, Stryer L, Baylor DA. 1988. Gating kinetics of the cyclic-GMP-activated channel of retinal rods: flash photolysis and voltage-jump studies. Proc Natl Acad Sci U.S.A., 85 (4):1287-1291.

Karpen JW, Zimmerman, A.L., Stryer, L., Baylor, D.A. 1988. Gating kinetics of the cyclic-GMP-activated channel of retinal rods: flash photolysis and voltage-jump studies. Proc Natl Acad Sci U.S.A., 85 (4):1287-1291.

Kaupp UB, Seifert R. 2001. Molecular diversity of pacemaker ion channels. Annu Rev Physiol, 63:235-257.

Kaupp UB, Seifert R. 2002. Cyclic nucleotide-gated ion channels. Physiol Rev, 82 (3):769-824.

Kaupp UB, Niidome T, Tanabe T, Terada S, Bonigk W, Stuhmer W, Cook NJ, Kangawa K, Matsuo H, Hirose T, et al. 1989. Primary structure and functional expression from complementary DNA of the rod photoreceptor cyclic GMP-gated channel. Nature, 342 (6251):762-766.

Kelliher KR, Ziesmann J, Munger SD, Reed RR, Zufall F. 2003. Importance of the CNGA4 channel gene for odor discrimination and adaptation in behaving mice. Proc Natl Acad Sci U.S.A., 100 (7):4299-4304.

Kirsch GE, Pascual JM, Shieh CC. 1995. Functional role of a conserved aspartate in the external mouth of voltage-gated potassium channels. Biophys J, 68 (5):1804-1813.

Kleene SJ. 2000. Spontaneous gating of olfactory cyclic-nucleotide-gated channels. J Membr Biol, 178 (1):49-54.

Kleene SJ, Gesteland RC. 1991. Calcium-activated chloride conductance in frog olfactory cilia. J Neurosci, 11 (11):3624-3629.

Komatsu H, Mori, I., Rhee, J.S., Akaike, N., Ohshima, Y. 1996. Mutations in a cyclic nucleotide-gated channel lead to abnormal thermosensation and chemosensation in C. elegans. Neuron, 17 (4):707-718.

Korschen HG, Illing M, Seifert R, Sesti F, Williams A, Gotzes S, Colville C, Muller F, Dose A, Godde M, et al. 1995. A 240 kDa protein represents the complete beta subunit of the cyclic nucleotide-gated channel from rod photoreceptor. Neuron, 15 (3):627-636.

Koshland DE, Jr., Nemethy G, Filmer D. 1966. Comparison of experimental binding data and theoretical models in proteins containing subunits. Biochemistry, 5 (1):365-385.

Kurahashi T, Menini A. 1997. Mechanism of odorant adaptation in the olfactory receptor cell. Nature, 385 (6618):725-729.

Kusch J, Zimmer T, Holschuh J, Biskup C, Schulz E, Nache V, Benndorf K. 2010a. Role of the S4-S5 linker in CNG channel activation. Biophys J, 99 (8):2488-2496.

Kusch J, Biskup C, Thon S, Schulz E, Nache V, Zimmer T, Schwede F, Benndorf K. 2010b. Interdependence of receptor activation and ligand binding in HCN2 pacemaker channels. Neuron, 67 (1):75-85.

Kusch J, Thon S, Schulz E, Biskup C, Nache V, Zimmer T, Seifert R, Schwede F, Benndorf K. 2012. How subunits cooperate in cAMP-induced activation of homotetrameric HCN2 channels. Nat Chem Biol, 8 (2):162-169.

Lee TE, Philipson LH, Nelson DJ. 1996. N-type inactivation in the mammalian Shaker K^+ channel Kv1.4. J Membr Biol, 151 (3):225-235.

Li J, Lester HA. 1999. Single-channel kinetics of the rat olfactory cyclic nucleotide-gated channel expressed in Xenopus oocytes. Mol Pharmacol, 55 (5):883-893.

Liman ER, Buck LB. 1994. A second subunit of the olfactory cyclic nucleotide-gated channel confers high sensitivity to cAMP. Neuron, 13 (3):611-621.

Liman ER, Tytgat J, Hess P. 1992. Subunit stoichiometry of a mammalian K^+ channel determined by construction of multimeric cDNAs. Neuron, 9 (5):861-871.

Liu DT, Tibbs GR, Siegelbaum SA. 1996. Subunit stoichiometry of cyclic nucleotide-gated channels and effects of subunit order on channel function. Neuron, 16 (5):983-990.

Liu DT, Tibbs GR, Paoletti P, Siegelbaum SA. 1998. Constraining ligand-binding site stoichiometry suggests that a cyclic nucleotide-gated channel is composed of two functional dimers. Neuron, 21 (1):235-248.

Ludwig J, Margalit T, Eismann E, Lancet D, Kaupp UB. 1990. Primary structure of cAMP-gated channel from bovine olfactory epithelium. FEBS Lett, 270 (1-2):24-29.

Mandiyan VS, Coats JK, Shah NM. 2005. Deficits in sexual and aggressive behaviors in Cnga2 mutant mice. Nat Neurosci, 8 (12):1660-1662.

Mathai JC, Agre P. 1999. Hourglass pore-forming domains restrict aquaporin-1 tetramer assembly. Biochemistry, 38 (3):923-928.

McCormack K, Joiner WJ, Heinemann SH. 1994. A characterization of the activating structural rearrangements in voltage-dependent Shaker K^+ channels. Neuron, 12 (2):301-315.

McCormack K, Lin L, Iverson LE, Tanouye MA, Sigworth FJ. 1992. Tandem linkage of Shaker K^+ channel subunits does not ensure the stoichiometry of expressed channels. Biophys J, 63 (5):1406-1411.

McCormack K, Tanouye MA, Iverson LE, Lin JW, Ramaswami M, McCormack T, Campanelli JT, Mathew MK, Rudy B. 1991. A role for hydrophobic residues in the voltage-dependent gating of Shaker K^+ channels. Proc Natl Acad Sci U S A, 88 (7):2931-2935.

Menini A. 1999. Calcium signalling and regulation in olfactory neurons. Curr Opin Neurobiol, 9 (4):419-426.

Michalakis S, Reisert J, Geiger H, Wetzel C, Zong X, Bradley J, Spehr M, Huttl S, Gerstner A, Pfeifer A, Hatt H, Yau KW, Biel M. 2006. Loss of CNGB1 protein leads

to olfactory dysfunction and subciliary cyclic nucleotide-gated channel trapping. J Biol Chem, 281 (46):35156-35166.

Minier F, Sigel E. 2004. Techniques: Use of concatenated subunits for the study of ligand-gated ion channels. Trends Pharmacol Sci, 25 (9):499-503.

Monod J, Wyman J, Changeux JP. 1965. On the nature of allosteric transitions: A plausible model. J Mol Biol, 12:88-118.

Morrill JA, MacKinnon R. 1999. Isolation of a single carboxyl-carboxylate proton binding site in the pore of a cyclic nucleotide-gated channel. J Gen Physiol, 114 (1):71-83.

Munger SD, Lane AP, Zhong H, Leinders-Zufall T, Yau KW, Zufall F, Reed RR. 2001. Central role of the CNGA4 channel subunit in Ca^{2+}-calmodulin-dependent odor adaptation. Science, 294 (5549):2172-2175.

Nache V, Eick T, Schulz E, Schmauder R, Benndorf K. 2013. Hysteresis of ligand binding in CNGA2 ion channels. Nat Commun, 4:2864.

Nache V, Schulz E, Zimmer T, Kusch J, Biskup C, Koopmann R, Hagen V, Benndorf K. 2005. Activation of olfactory-type cyclic nucleotide-gated channels is highly cooperative. J Physiol, 569 (Pt 1):91-102.

Nache V, Zimmer T, Wongsamitkul N, Schmauder R, Kusch J, Reinhardt L, Bonigk W, Seifert R, Biskup C, Schwede F, Benndorf K. 2012. Differential regulation by cyclic nucleotides of the CNGA4 and CNGB1b subunits in olfactory cyclic nucleotide-gated channels. Sci Signal, 5 (232):ra48.

Nakamura T, Gold GH. 1987. A cyclic nucleotide-gated conductance in olfactory receptor cilia. Nature, 325 (6103):442-444.

Neher E, Sakmann B. 1976. Single-channel currents recorded from membrane of denervated frog muscle fibres. Nature, 260 (5554):799-802.

Newbolt A, Stoop R, Virginio C, Surprenant A, North RA, Buell G, Rassendren F. 1998. Membrane topology of an ATP-gated ion channel (P2X receptor). J Biol Chem, 273 (24):15177-15182.

Nicke A, Rettinger J, Schmalzing G. 2003. Monomeric and dimeric byproducts are the principal functional elements of higher order P2X1 concatamers. Mol Pharmacol, 63 (1):243-252.

Paoletti P, Young EC, Siegelbaum SA. 1999. C-Linker of cyclic nucleotide-gated channels controls coupling of ligand binding to channel gating. J Gen Physiol, 113 (1):17-34.

Peng C, Rich ED, Varnum MD. 2004. Subunit configuration of heteromeric cone cyclic nucleotide-gated channels. Neuron, 42 (3):401-410.

Pessia M, Tucker SJ, Lee K, Bond CT, Adelman JP. 1996. Subunit positional effects revealed by novel heteromeric inwardly rectifying K^+ channels. EMBO J, 15 (12):2980-2987.

Pfeifer A, Ruth P, Dostmann W, Sausbier M, Klatt P, Hofmann F. 1999. Structure and function of cGMP-dependent protein kinases. Rev Physiol Biochem Pharmacol, 135:105-149.

Picones A, Korenbrot JI. 1995. Spontaneous, ligand-independent activity of the cGMP-gated ion channels in cone photoreceptors of fish. J Physiol, 485 (Pt 3):699-714.

Press WHT, S.A.; Vetterling, W.T.; Flannery, B.P. 2002. Numerical Recipes in C: The Art of Scientific Computing. Cambridge University Press (2^{nd} ed.):685.

Ruiz M, Karpen JW. 1999. Opening mechanism of a cyclic nucleotide-gated channel based on analysis of single channels locked in each liganded state. J Gen Physiol, 113 (6):873-895.

Sack JT, Shamotienko O, Dolly JO. 2008. How to validate a heteromeric ion channel drug target: assessing proper expression of concatenated subunits. J Gen Physiol, 131 (5):415-420.

Sahin-Toth M, Lawrence MC, Kaback HR. 1994. Properties of permease dimer, a fusion protein containing two lactose permease molecules from Escherichia coli. Proc Natl Acad Sci U.S.A., 91 (12):5421-5425.

Sautter A, Zong X, Hofmann F, Biel M. 1998. An isoform of the rod photoreceptor cyclic nucleotide-gated channel beta subunit expressed in olfactory neurons. Proc Natl Acad Sci U.S.A., 95 (8):4696-4701.

Schachtman DP. 2000. Molecular insights into the structure and function of plant $K^{(+)}$ transport mechanisms. Biochim Biophys Acta, 1465 (1-2):127-139.

Schoppa NE, McCormack K, Tanouye MA, Sigworth FJ. 1992. The size of gating charge in wild-type and mutant Shaker potassium channels. Science, 255 (5052):1712-1715.

Shapiro MS, Zagotta WN. 1998. Stoichiometry and arrangement of heteromeric olfactory cyclic nucleotide-gated ion channels. Proc Natl Acad Sci U.S.A., 95 (24):14546-14551.

Silverman SK, Lester HA, Dougherty DA. 1996. Subunit stoichiometry of a heteromultimeric G protein-coupled inward-rectifier K^+ channel. J Biol Chem, 271 (48):30524-30528.

Sokolov MV, Shamotienko O, Dhochartaigh SN, Sack JT, Dolly JO. 2007. Concatemers of brain Kv1 channel alpha subunits that give similar K^+ currents yield pharmacologically distinguishable heteromers. Neuropharmacology, 53 (2):272-282.

Spehr M, Wetzel CH, Hatt H, Ache BW. 2002. 3-phosphoinositides modulate cyclic nucleotide signaling in olfactory receptor neurons. Neuron, 33 (5):731-739.

Stelmashenko O, Lalo U, Yang Y, Bragg L, North RA, Compan V. 2012. Activation of trimeric P2X2 receptors by fewer than three ATP molecules. Mol Pharmacol, 82 (4):760-766.

Strunker T, Weyand I, Bonigk W, Van Q, Loogen A, Brown JE, Kashikar N, Hagen V, Krause E, Kaupp UB. 2006. A K^+-selective cGMP-gated ion channel controls chemosensation of sperm. Nat Cell Biol, 8 (10):1149-1154.

Tanaka JC, Eccleston JF, Furman RE. 1989. Photoreceptor channel activation by nucleotide derivatives. Biochemistry, 28 (7):2776-2784.

Tibbs GR, Goulding EH, Siegelbaum SA. 1997. Allosteric activation and tuning of ligand efficacy in cyclic-nucleotide-gated channels. Nature, 386 (6625):612-615.

Tibbs GR, Liu DT, Leypold BG, Siegelbaum SA. 1998. A state-independent interaction between ligand and a conserved arginine residue in cyclic nucleotide-gated channels reveals a functional polarity of the cyclic nucleotide binding site. J Biol Chem, 273 (8):4497-4505.

Tu L, Deutsch C. 1999. Evidence for dimerization of dimers in K^+ channel assembly. Biophys J, 76 (4):2004-2017.

Tytgat J, Hess P. 1992. Evidence for cooperative interactions in potassium channel gating. Nature, 359 (6394):420-423.

Tytgat J, Nakazawa K, Gross A, Hess P. 1993. Pursuing the voltage sensor of a voltage-gated mammalian potassium channel. J Biol Chem, 268 (32):23777-23779.

Ulens C, Siegelbaum SA. 2003. Regulation of hyperpolarization-activated HCN channels by cAMP through a gating switch in binding domain symmetry. Neuron, 40 (5):959-970.

Varnum MD, Zagotta WN. 1996. Subunit interactions in the activation of cyclic nucleotide-gated ion channels. Biophys J, 70 (6):2667-2679.

Wang R, Su J, Wang X, Piao H, Zhang X, Adams CY, Cui N, Jiang C. 2005. Subunit stoichiometry of the Kir1.1 channel in proton-dependent gating. J Biol Chem, 280 (14):13433-13441.

Weber IT, Gilliland GL, Harman JG, Peterkofsky A. 1987. Crystal structure of a cyclic AMP-independent mutant of catabolite gene activator protein. J Biol Chem, 262 (12):5630-5636.

Weitz D, Ficek N, Kremmer E, Bauer PJ, Kaupp UB. 2002. Subunit stoichiometry of the CNG channel of rod photoreceptors. Neuron, 36 (5):881-889.

White MM. 2006. Pretty subunits all in a row: using concatenated subunit constructs to force the expression of receptors with defined subunit stoichiometry and spatial arrangement. Mol Pharmacol, 69 (2):407-410.

White MM, Aylwin M. 1990. Niflumic and flufenamic acids are potent reversible blockers of Ca^{2+}-activated Cl^- channels in Xenopus oocytes. Mol Pharmacol, 37 (5):720-724.

Yan C, Zhao AZ, Bentley JK, Loughney K, Ferguson K, Beavo JA. 1995. Molecular cloning and characterization of a calmodulin-dependent phosphodiesterase

enriched in olfactory sensory neurons. Proc Natl Acad Sci U.S.A., 92 (21):9677-9681.

Yang J, Jan YN, Jan LY. 1995. Determination of the subunit stoichiometry of an inwardly rectifying potassium channel. Neuron, 15 (6):1441-1447.

Zagotta WN, Siegelbaum SA. 1996. Structure and function of cyclic nucleotide-gated channels. Annu Rev Neurosci, 19:235-263.

Zerhusen B, Zhao J, Xie J, Davis PB, Ma J. 1999. A single conductance pore for chloride ions formed by two cystic fibrosis transmembrane conductance regulator molecules. J Biol Chem, 274 (12):7627-7630.

Zheng C, Feinstein P, Bozza T, Rodriguez I, Mombaerts P. 2000. Peripheral olfactory projections are differentially affected in mice deficient in a cyclic nucleotide-gated channel subunit. Neuron, 26 (1):81-91.

Zheng J, Zagotta WN. 2004. Stoichiometry and assembly of olfactory cyclic nucleotide-gated channels. Neuron, 42 (3):411-421.

Zheng J, Trudeau MC, Zagotta WN. 2002. Rod cyclic nucleotide-gated channels have a stoichiometry of three CNGA1 subunits and one CNGB1 subunit. Neuron, 36 (5):891-896.

Zhong H, Molday LL, Molday RS, Yau KW. 2002. The heteromeric cyclic nucleotide-gated channel adopts a 3A:1B stoichiometry. Nature, 420 (6912):193-198.

Zhou L, Olivier NB, Yao H, Young EC, Siegelbaum SA. 2004. A conserved tripeptide in CNG and HCN channels regulates ligand gating by controlling C-terminal oligomerization. Neuron, 44 (5):823-834.

Zhou Y, Nelson ME, Kuryatov A, Choi C, Cooper J, Lindstrom J. 2003. Human alpha4beta2 acetylcholine receptors formed from linked subunits. J Neurosci, 23 (27):9004-9015.

Zong X, Zucker H, Hofmann F, Biel M. 1998. Three amino acids in the C-linker are major determinants of gating in cyclic nucleotide-gated channels. EMBO J, 17 (2):353-362.

Zufall F, Firestein S, Shepherd GM. 1991. Analysis of single cyclic nucleotide-gated channels in olfactory receptor cells. J Neurosci, 11 (11):3573-3580.

Abbreviation

AC	adenylyl cyclase
Ag/AgCl	Silver/Silver chloride
ClC_{Ca}	Ca^{2+}- activated Cl^- channel
CaM	Calmodulin
cAMP	adenosine 3':5'-cyclic monophosphate
CD model	coupled dimer model
CFTR	Cystic Fibrosis Transmembrane Conductance Regulator
cGMP	guanosine 3':5'-cyclic monophosphate
CNBD	cyclic nucleotide-binding domain
CNG channels	cyclic nucleotide-gated channels
cRNA	complementary RNA
EC_{50}	concentration of the cyclic nucleotide that activates 50% of maximum current
ENaC	epithelial Na^+ channels
EOG	electroolfactrogram recordings
FRET	fluorescence resonance energy transfer
G_{olf}	G-protein olfactory specific subtype
H	Hill coefficient
HCN	hyperpolarization-activated cyclic nucleotide-gated channels
HERG	human eag-related gene family of K^+ channels
I	current (pA)
I_{max}	maximum current
mM	Millimolar

MWC	Monod-Wyman-Changeux model
NCX	Na^+-Ca^{2+} exchanger
PIP_3	phosphatidylinositol-3,4,5-trisphosphate
P_o	Open probability
PDE	phosphodiesterase
PKA	cAMP - dependent protein kinases
PKG	cGMP- dependent protein kinases
OR	odorant receptor
OSNs	olfactory sensory neurons
K_v	voltage-gated K^+ channels
μM	Micromolar

Curriculum Vitae

Name: Nisa Wongsamitkul

Place and Date of birth: Saraburi/Thailand, 08.09.1983

Address: 07743 Jena, Gartenstr. 5

Nationality: Thai

E-mail: Nisa.wongsamitkul@yahoo.com

Telephone: +49-(0)152-52122708

Education

Ph.D. in Natural Science 2010-2015

- Institut für Physiologie II, Universitätsklinikum Jena, Germany
- IZKF Graduate Program Experimental Medicine
    - Thesis title: Translation of ligand binding to channel activation in olfactory cyclic nucleotide-gated (CNG) channels.

M.Sc. in Toxicology 2006-2009

- Faculty of Science, Mahidol University, Bangkok, Thailand
    - Project title**:** Effect of tannin on the function of CFTR chloride channel.

B.Sc. in Biology (2^{nd} honor) 2002-2006

- Faculty of Science, Silpakorn University, Nakornpathom, Thailand
    - Project title**:** Screening for potential *Bacillus* spp. for the control of *Trichoderma* spp. infected the culture of shiitake mushroom *Lentinus edodes.*

Publications

Wongsamitkul, N., Nache, V., Eick, T., Hummert, S., Schulz, E., Schmauder, R.,Weiser, N., Schirmeyer, J., Zimmer, T., Benndorf, K. Dissecting the work of a single subunit in a tetrameric CNGA2 ion channel.
(Articles submitted for publication to Nature Communications)

Nache, V., Zimmer, T., **Wongsamitkul, N.**, Schmauder, R., Kusch, J., Reinhardt, L., Bönigk, W., Seifert, R., Biskup, C., Schwede, F., Benndorf, K. Differential Regulation by Cyclic Nucleotides of the CNGA4 and CNGB1b Subunits in Olfactory Cyclic Nucleotide-Gated Channels. Science Signaling. 2012 Jul 10; 5(232):ra48.

Wongsamitkul, N., Sirianant, L., Muanprasat, C., Chatsudthipong, V. A plant-derived hydrolysable tannin inhibits CFTR chloride channel: a potential treatment of diarrhea. Pharmaceutical Research. 2010 March; 27(3):490-7.

Chittihunsa, T., Bangeekhan, E., **Wongsamitkul, N.**, Subsomboon, T. Screening of *Bacillus* spp. Suppressing the infection of *Trichoderma* sp. in mushroom cultivation. KMITL Science and Technology Journal. 2007 Nov; 7 No. S1.

Presentations

Nache, V., **Wongsamitkul, N.,** Zimmer, T., Benndorf, K. Effect of ligand binding to the B1b subunit of olfactory CNG channels. 59th Biophysical Society Annual Meeting, Feb 7th-11st, 2015, in Baltimore, Maryland, USA.

Wongsamitkul, N., Nache, V., Schmauder, R., Eberhard M., Weiser, N., Zimmer, T., Benndorf, K. Characterization of the olfactory CNG-channel gating at the single-channel level. 93nd Annual Meeting of the German Physiological Society, DPG, March 13nd - 15th, 2014, Mainz, Germany.

Wongsamitkul, N., Nache, V., Zimmer, T., Benndorf, K. Monitoring the work of a single subunit in homotetrameric CNGA2 channels. 92nd Annual Meeting of the German Physiological Society, DPG, March 2nd - 5th, 2013, in Heidelberg, Germany.

Nache, V., **Wongsamitkul, N.,** Schmauder, R., Eberhard M., Weiser, N., Zimmer, T., Benndorf, K. Elucidating the contribution of cNGA4 and CNGB1b subunits to the CNG-channel gating: A single-channel study. 56th Biophysical Society Annual Meeting, Feb 25th-29th, 2012, in Sanfrancisco, California, U.S.A.

Nache, V., **Wongsamitkul, N.,** Schulz, E., Zimmer, T., Kusch J., Schwede F., Benndorf, K. Kinetic study of ligand-induced activation in homo-and heterotetrameric olfactory CNG channels. 55th Biophysical Society Annual Meeting, March 5th - 9th, 2011, in Baltimore, Maryland, U.S.A.

Acknowledgements

First and foremost, I would like to express the deepest appreciation to my major advisor, Prof. Klaus Benndorf. He has been supportive since the days that I had a great opportunity to have an interview with him at Institute for Physiology II. Although, the time of interview was short but I still remembered the wonderful interview day with him. He asked me with large smiling which project will you like to work and he introduced me to everyone in his lab. This made me felt like home in the institute. From the early state of my research project until my thesis defense, he taught me how to enrich with ideas and scientific passions, thereby inspiring me to pursue my future career in science.

I also wish to thank my special advisor, Dr. Vasilica Nache, who has supported me not only by providing research guidance but also by suggesting me in academic and personal problems through the rough road to finish my thesis over almost four years. I have felt like I always had a sister beside me every day when I went to work. She has been source of supervision, excellent advice and caring during the most difficult time when I had to hurry to finish my thesis in which I need to move on. Without her generous guidance and persistent assistance this dissertation would have not been successful. I also would like to thank Prof. Dr. Thomas Zimmer and Karin Schoknecht for all concatemeric constructs, Dr. Thomas Eick and Sabine Hummert for performing Markovian models. In addition, I am hugely indebted to Dr. Jana Kusch for reading my dissertation and I am grateful to Dominik Lenz for helping me in my German summary part.

Also, I sincerely thank to all of my beloved colleagues who helped and suggested me several techniques and scientific knowledge both. Moreover, I want to express my sincere gratitude to my thesis committee members who carefully corrected my thesis and offered me brilliant suggestions for the oral defense. Lastly, I praise the enormous amount of energy and love from my family; mother, father, younger brother and grandmother in Thailand.

Ehrenwörtliche Erklärung

hiermit erkläre ich, dass mir die Promotionsordnung der Medizinischen Fakultät der Friedrich-Schiller-Universität bekannt ist, ich die Dissertation selbst angefertigt habe und alle von mir benutzten Hilfsmittel, persönlichen Mitteilungen und Quellen in meiner Arbeit angegeben sind,

mich folgende Personen bei der Auswahl und Auswertung des Materials sowie bei der Herstellung des Manuskripts unterstützt haben: Prof. Dr. Klaus Benndorf, Prof. Dr. Ingo Dahse, Dr. Vasilica Nache

die Hilfe eines Promotionsberaters nicht in Anspruch genommen wurde und dass Dritte weder unmittelbar noch mittelbar geldwerte Leistungen von mir für Arbeiten erhalten haben, die in Zusammenhang mit dem Inhalt der vorgelegten Dissertation stehen,

dass ich die Dissertation noch nicht als Prüfungsarbeit für eine staatliche oder andere wissenschaftliche Prüfungen eingereicht habe und

dass ich die gleiche, eine in wesentlichen Teilen ähnliche oder eine andere Abhandlung nicht bei einer anderen Hochschule als Dissertation eingereicht habe.

Jena, 28.01.2015 Nisa Wongsamitkul